Results

Patient characteristics

Among the 25 patients enrolled at the University of Tokyo Hospital, 15 met all of the inclusion criteria. The reasons for exclusion included insufficient tumor marker determination prior to TSU-68 administration (seven patients), results of CT prior to enrollment unavailable (one patient), no tumor marker elevation (one patient), and termination of TSU-68 administration at week 2 as a result of gastrointestinal bleeding (one patient). The baseline characteristics of the 15 patients included in the current study cohort are summarized in Table 1.

Table 1 Patient characteristics

Variable	$n = 15$
Age (years)	66.7 ± 6.3
Sex [no. (%)]	
Male	12 (80)
Female	3 (20)
Viral markers [no. (%)]	
HBs Ag+, HCV Ab−	2 (13)
HBs Ag−, HCV Ab+	13 (87)
Prior treatments[a] [no. (%)]	
TACE	13 (87)
Ablation	12 (80)
Surgery	5 (33)
Radiation	2 (13)
Systemic chemotherapy	1 (7)
Tumor stage [no. (%)[b]]	
I	0 (0)
II	0 (0)
III	7 (47)
IVa	4 (27)
IVb	4 (27)
Extrahepatic metastasis [no. (%)]	8 (53)
Portal vein thrombosis [no. (%)]	1 (7)

Plus-minus values represent the mean and standard deviation

HBs Ag hepatitis B surface antigen, *HCV Ab* hepatitis C antibody

[a] Number of pretreatments by surgery, radiofrequency ablation, transcatheter arterial chemoembolization, chemotherapy, or radiotherapy

[b] Based on the International Union Against Cancer (UICC) *TNM Classification of Malignant Tumors*, 6th edition, 2002

Tumor volume and tumor marker prior to TSU-68 administration

The relationship between the tumor volume and tumor marker DTs is shown in Fig. 2, where each point represents data from one patient. With the least-square method, the relationship was regressed to

$$y = 1.063x - 2.941$$

where x is the tumor volume DT and y is the tumor marker DT in days for both. The slope of regression was close to 1.0 with an r^2 value of 0.948, indicating that these two DTs were almost identical in each patient.

Changes in tumor marker DT during TSU-68 treatment

TSU-68 treatment was discontinued at week 4 in four patients because of the appearance of new lesions or a substantial increase in the volume of non-target lesions. The remaining 11 patients received this drug for at least 8 weeks and the response of the target lesions was evaluated in these patients as a stable disease (SD) by RECIST at week 4. Changes in the tumor marker DT before and after the commencement of TSU-68 administration are summarized in Table 2, together with the corresponding RECIST evaluation. When the tumor marker DT was increased following TSU-68 therapy, or became negative, this was considered to be an indication of at least partial drug efficacy. On the other hand, no beneficial effects were assigned to TSU-68 when the tumor marker DT was shortened following treatment. Such tumor marker-based evaluations were found to be compatible with RECIST, as a complete or partial response (CR, PR), or SD versus PD, in 12 of 15 patients. In the remaining three patients, a RECIST-based evaluation of PD was obtained in spite of an elongated tumor marker DT. In case 9, the RECIST-based evaluation became PD after cycle 2 because of the appearance of a new lesion, although the tumor marker DT was still elongated in this patient. Lymph node necrosis was observed by contrast-enhanced CT in this patient (Fig. 3), suggesting that TSU-68 remained effective. In case 10, a RECIST-based evaluation of PD was obtained because of an increase in the size of adrenal metastasis (a target lesion) although the hepatic lesions were decreased in size and the tumor marker DT was elongated. After the cessation of TSU-68 in patient 10, the left adrenal gland was excised and found to contain multiple necrotic lesions. Case 12 showed SD for the target lesion and an elongated tumor marker DT but was deemed to be a PD because of the appearance of new lesions.

In two of the other cases (nos. 1 and 2), a RECIST-based evaluation of SD was found but a negative tumor marker DT was also obtained. In case 1, the tumor marker DT became −21.1 days upon TSU-86 administration, which indicated an 84% decrease in tumor volume and 46% reduction in diameter by 8 weeks. Using RECIST parameters, a greater than 30% decrease in diameter typically corresponds to PR but case 1 was nevertheless evaluated as

SD using this system. In case 2, a tumor marker DT of −29.5 days corresponded to a decrease in diameter to 64% of baseline but the RECIST-based evaluation was SD. Importantly, necrotic lesions were found in the target tumors in both cases, possibly leading to an underestimation of anticancer effect.

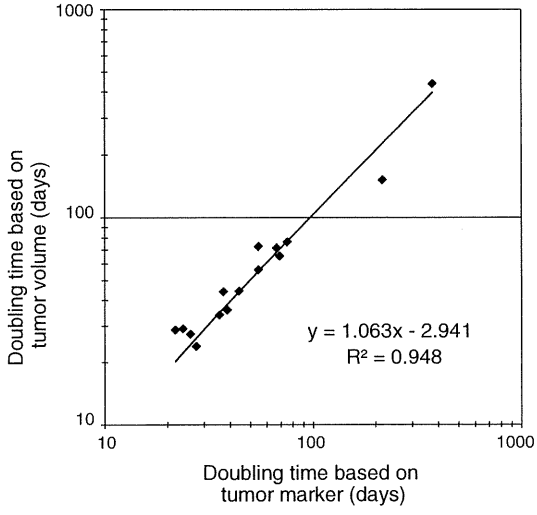

Fig. 2 Linear regression representation of the log tumor volume doubling time over the log tumor marker doubling time. *Each point* represents a data set from a single patient

Changes in tumor marker DT after the cessation of TSU-68 treatment

Changes in tumor marker DTs following the cessation of TSU-68 could be evaluated in four patients (Table 3). In each of these cases, the tumor marker DTs were elongated during TSU-68 administration compared with the baseline value and became shorter after the cessation of the treatment. Tumor marker DT after the cessation of TSU-68 was comparable with that before treatment in three patients and shorter in the remaining case.

Discussion

The production rate of a tumor marker per unit volume of the tumor mass can vary greatly among cancer patients who are positive for this marker. Hence, the serum levels of tumor marker are not directly proportional to the tumor volume. However, provided that the production rate per unit of tumor volume remains constant in each case, the changes in the serum tumor marker levels will directly correspond to the changes in tumor volume. Indeed, as we have shown in the present study, the DT of a tumor marker level and that of the corresponding tumor volume were almost identical in each patient in this study, at least during

Table 2 Tumor marker doubling time and treatment response evaluated by RECIST

Case no.	Marker	Tumor marker levels[a]		Doubling time (days)		Treatment response by RECIST
		At enrollment	At evaluation	During washout phase	During TSU-68 administration	
1	DCP	213	29	136.8	−21.1[b]	SD
2	AFP	60836	15312	38.6	−29.5[b]	SD
3	DCP	5993	5007	26.9	−231.6[b]	SD
4	AFP	144045	134030	75.3	−602.1[b]	SD
5	AFP	12004	12010	18.8	43004	SD
6	AFP	33859	33983	24.1	3010	SD[c]
7	AFP	61649	88056	71.7	115.8	SD
8	AFP	198	395	51.9	60.2	SD
9	AFP	45	92	28.0	60.2	PD
10	DCP	657	997	38.1	51.0	PD[c]
11	DCP	3188	8275	54.7	43.6	PD
12	AFP	3404	6430	24.7	32.4	PD[c]
13	AFP	53	203	88.5	15.5	PD[c]
14	AFP	19	544	376.3	12.4	PD
15	AFP	30	169	25.7	12.0	PD[c]

AFP alpha-fetoprotein, *DCP* des-gamma carboxyprothrombin, *SD* stable disease, *PD* progressive disease

[a] Unit of AFP is ng/ml and unit of DCP is mAu/ml

[b] Became negative when the tumor marker levels decreased following treatment; negative DT values correspond to the half-life

[c] Calculated using the values obtained at week 4 as treatment was discontinued at this time point. The treatment response evaluations using RECIST were also performed at week 4

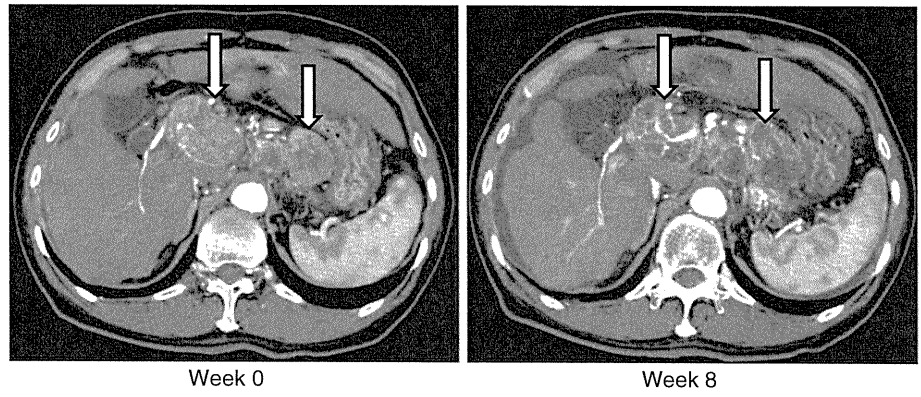

Fig. 3 A case in which a RECIST evaluation of PD was obtained even though the tumor marker levels had decreased. The lymph nodes around the hepatic arteries (target lesions, *arrows*) in this patient were enlarged and had become internally necrotic

Table 3 Tumor marker doubling time (days) before, during, and after TSU-68 treatment

Case no.	During washout phase	During the first 4 weeks of administration	During the last 4 weeks of administration	After cessation of administration
3	26.9	−97.1[b]	91.2	41.2
4	75.3	−79.2[b]	188.1	17.8
6[a]	24.1	3010	–	46.3
9	28.0	60.2	60.2	35.4

[a] Treatment was discontinued at week 4

[b] Became negative when the tumor marker levels decreased following treatment

washout phase prior to TSU-68 therapy. This indicates the possibility that tumor growth rates and any changes in them can be evaluated using tumor marker DT.

To validate the usefulness of tumor marker DTs for evaluating treatment responses, we compared this approach with the RECIST guidelines during TSU-68 administration. These two methods showed comparable results in most cases (12/15) and discrepancies were due to substantial tumor necrosis without volume shrinkage or to the appearance of new lesions in spite of the sustained effects of the drug on the target lesions. Tumor marker levels can be considered to represent viable tumor burden irrespective of the presence of necrosis or fibrosis. Evaluations based on tumor marker DTs may thus provide a better assessment of the efficacy of chemotherapeutic agents. Modified RECIST was proposed after the protocol of this study was completed. In modified RECIST, only areas with hyperattenuation were measured, excluding necrotic tissues. Modified RECIST was reported to be more useful than conventional RECIST in the evaluation of antiangiogenic agents. Although we did not directly compare tumor DT with modified RECIST in the present study, assessment based on tumor DT may be closer to modified RECIST than to conventional RECIST.

In several previous papers, early changes in AFP levels were used to assess responses to HCC treatments [30–32]. However, they evaluated only initial responses to therapy. In contrast, by evaluating tumor DT based on tumor marker levels, the effectiveness of a therapeutic agent can be monitored during its administration even when it changes over time.

In previous phase III trials of sorafenib, the response rate was not high but the overall survival was significantly improved [33, 34]. Slowing down the progression of a tumor, even if there is no reduction in the tumor volume, can therefore lead to prolonged survival. In the present study, the tumor marker DT was shortened after the cessation of TSU-68 treatment in four patients, i.e., tumor growth was accelerated, indicating that TSU-68 still inhibited tumor growth. Using RECIST evaluation, however, the treatment response in such cases will be judged as a PD, because this method does not consider time. Hence, in evaluating the response to cytostatic agents in particular, such as sorafenib and TSU-68, determination of the changes in the tumor growth rate may be substantially more adequate. Tumor marker levels can be easily measured repeatedly and, as shown in the current analysis, the corresponding DTs can thus be reliably calculated. Theoretically, the serum half-life of a tumor marker may affect the calculation of tumor DT. However, the half-life of AFP is 5 days and that of DCP is 40 h, which are much shorter than the tumor halving time even when TSU-68 is effective, and are negligible in calculations.

Another application of tumor marker DTs is the estimation of tumor growth rates when the lesions are untreated. DTs may correlate with the malignant potential of the tumor. We have shown that tumor marker DTs remained similar before the administration and after the cessation of TSU-68, which may be a characteristic of cytostatic agents in contrast to cytotoxic agents [35–37]. The decision to continue cytotoxic agents that only slow down tumor growth could be partially based on the tumor marker DT prior to treatment.

There are several limitations to the use of tumor marker DTs in the evaluation of cancer drug treatment responses. First, DTs cannot be calculated when a tumor does not produce tumor markers. Second, a tumor marker profile may change during treatment, possibly as a result of somatic mutation and clonal selection in the tumor cell population. This may make interpretation of changes in DTs difficult. Lastly, whether an elongated but still positive DT is associated with improved prognosis has yet to be confirmed. In the natural course of HCC, the tumor volume DT has been reported to be associated with prognosis [38]. We thus speculate that a treatment associated with elongation of tumor marker DT can be continued if there are no alternative treatments and the side effects are tolerable.

In conclusion, we have shown that serum tumor marker levels can be used to evaluate viable tumor burden irrespective of the presence of tumor necrosis that can compromise radiographic evaluations. This may be particularly useful in the evaluation of cytostatic agents.

Conflict of interest The authors declare that they have no conflict of interest.

References

1. Cannistra SA. Phase II trials in *Journal of Clinical Oncology*. J Clin Oncol. 2009;27:3073–6.
2. Paesmans M, Sculier JP, Libert P, Bureau G, Dabouis G, Thiriaux J, et al. Response to chemotherapy has predictive value for further survival of patients with advanced non-small cell lung cancer: 10 years experience of the European Lung Cancer Working Party. Eur J Cancer. 1997;33:2326–32.
3. Buyse M, Thirion P, Carlson RW, Burzykowski T, Molenberghs G, Piedbois P. Relation between tumour response to first-line chemotherapy and survival in advanced colorectal cancer: a meta-analysis. Meta-Analysis Group in Cancer. Lancet. 2000;356: 373–8.
4. Goffin J, Baral S, Tu D, Nomikos D, Seymour L. Objective responses in patients with malignant melanoma or renal cell cancer in early clinical studies do not predict regulatory approval. Clin Cancer Res. 2005;11:5928–34.
5. Keppke AL, Salem R, Reddy D, Huang J, Jin J, Larson AC, et al. Imaging of hepatocellular carcinoma after treatment with yttrium-90 microspheres. AJR Am J Roentgenol. 2007;188: 768–75.
6. Miller FH, Keppke AL, Reddy D, Huang J, Jin J, Mulcahy MF, et al. Response of liver metastases after treatment with yttrium-90 microspheres: role of size, necrosis, and PET. AJR Am J Roentgenol. 2007;188:776–83.
7. Burton A. REGIST: right time to renovate? Eur J Cancer. 2007;43:1642.
8. Therasse P, Eisenhauer EA, Buyse M. Update in methodology and conduct of cancer clinical trials. Eur J Cancer. 2006;42: 1322–30.
9. Therasse P, Eisenhauer EA, Verweij J. RECIST revisited: a review of validation studies on tumour assessment. Eur J Cancer. 2006;42:1031–9.
10. Stroobants S, Goeminne J, Seegers M, Dimitrijevic S, Dupont P, Nuyts J, et al. 18FDG-positron emission tomography for the early prediction of response in advanced soft tissue sarcoma treated with imatinib mesylate (Glivec). Eur J Cancer. 2003;39:2012–20.
11. Antoch G, Kanja J, Bauer S, Kuehl H, Renzing-Koehler K, Schuette J, et al. Comparison of PET, CT, and dual-modality PET/CT imaging for monitoring of imatinib (STI571) therapy in patients with gastrointestinal stromal tumors. J Nucl Med. 2004;45:357–65.
12. D'Amico AV, Desjardin A, Chen MH, Paik S, Schultz D, Renshaw AA, et al. Analyzing outcome-based staging for clinically localized adenocarcinoma of the prostate. Cancer. 1998;83:2172–80.
13. Sheu JC, Sung JL, Chen DS, Yang PM, Lai MY, Lee CS, et al. Growth rate of asymptomatic hepatocellular carcinoma and its clinical implications. Gastroenterology. 1985;89:259–66.
14. Tian F, Appert HE, Myles J, Howard JM. Prognostic value of serum CA 19-9 levels in pancreatic adenocarcinoma. Ann Surg. 1992;215:350–5.
15. Tanaka K, Noura S, Ohue M, Seki Y, Yamada T, Miyashiro I, et al. Doubling time of carcinoembryonic antigen is a significant prognostic factor after the surgical resection of locally recurrent rectal cancer. Dig Surg. 2008;25:319–24.
16. Stamey TA, Kabalin JN, Ferrari M. Prostate specific antigen in the diagnosis and treatment of adenocarcinoma of the prostate. III. Radiation treated patients. J Urol. 1989;141:1084–7.
17. Stamey TA, Kabalin JN, Ferrari M, Yang N. Prostate specific antigen in the diagnosis and treatment of adenocarcinoma of the prostate. IV. Anti-androgen treated patients. J Urol. 1989;141: 1088–90.
18. Stamey TA, Kabalin JN, McNeal JE, Johnstone IM, Freiha F, Redwine EA, et al. Prostate specific antigen in the diagnosis and treatment of adenocarcinoma of the prostate. II. Radical prostatectomy treated patients. J Urol. 1989;141:1076–83.
19. Fabbro D, Manley PW. Su-6668. SUGEN. Curr Opin Investig Drugs. 2001;2:1142–8.
20. Pang RW, Poon RT. From molecular biology to targeted therapies for hepatocellular carcinoma: the future is now. Oncology. 2007;72(Suppl 1):30–44.
21. Kanai F, Yoshida H, Tateishi R, Sato S, Kawabe T, Obi S, et al. A phase I/II trial of the oral antiangiogenic agent TSU-68 in patients with advanced hepatocellular carcinoma. Cancer Chemother Pharmacol. 2011;67:315–24.
22. Eisenhauer EA. Phase I and II trials of novel anti-cancer agents: endpoints, efficacy and existentialism. The Michel Clavel Lecture, held at the 10th NCI-EORTC Conference on New Drugs in Cancer Therapy, Amsterdam, 16–19 June 1998. Ann Oncol. 1998;9:1047–52.
23. Eisenhauer EA. Response evaluation: beyond RECIST. Ann Oncol. 2007;18 Suppl 9:ix29–32.
24. Gelmon KA, Eisenhauer EA, Harris AL, Ratain MJ, Workman P. Anticancer agents targeting signaling molecules and cancer cell environment: challenges for drug development? J Natl Cancer Inst. 1999;91:1281–7.
25. Korn EL, Arbuck SG, Pluda JM, Simon R, Kaplan RS, Christian MC. Clinical trial designs for cytostatic agents: are new approaches needed? J Clin Oncol. 2001;19:265–72.
26. Ratain MJ, Eckhardt SG. Phase II studies of modern drugs directed against new targets: if you are fazed, too, then resist RECIST. J Clin Oncol. 2004;22:4442–5.
27. Therasse P, Arbuck SG, Eisenhauer EA, Wanders J, Kaplan RS, Rubinstein L, et al. New guidelines to evaluate the response to treatment in solid tumors European Organization for Research and Treatment of Cancer, National Cancer Institute of the United States, National Cancer Institute of Canada. J Natl Cancer Inst. 2000;92:205–16.
28. Dachman AH, MacEneaney PM, Adedipe A, Carlin M, Schumm LP. Tumor size on computed tomography scans: is one measurement enough? Cancer. 2001;91:555–60.

29. Schwartz M. A biomathematical approach to clinical tumor growth. Cancer. 1961;14:1272–94.
30. Chan SL, Mo FK, Johnson PJ, Hui EP, Ma BB, Ho WM, et al. New utility of an old marker: serial alpha-fetoprotein measurement in predicting radiologic response and survival of patients with hepatocellular carcinoma undergoing systemic chemotherapy. J Clin Oncol. 2009;27:446–52.
31. Riaz A, Ryu RK, Kulik LM, Mulcahy MF, Lewandowski RJ, Minocha J, et al. Alpha-fetoprotein response after locoregional therapy for hepatocellular carcinoma: oncologic marker of radiologic response, progression, and survival. J Clin Oncol. 2009;27:5734–42.
32. Shao YY, Lin ZZ, Hsu C, Shen YC, Hsu CH, Cheng AL. Early alpha-fetoprotein response predicts treatment efficacy of antiangiogenic systemic therapy in patients with advanced hepatocellular carcinoma. Cancer. 2010;116:4590–6.
33. Llovet JM, Ricci S, Mazzaferro V, Hilgard P, Gane E, Blanc JF, et al. Sorafenib in advanced hepatocellular carcinoma. N Engl J Med. 2008;359:378–90.
34. Cheng AL, Kang YK, Chen Z, Tsao CJ, Qin S, Kim JS, et al. Efficacy and safety of sorafenib in patients in the Asia-Pacific region with advanced hepatocellular carcinoma: a phase III randomised, double-blind, placebo-controlled trial. Lancet Oncol. 2009;10:25–34.
35. Bourhis J, Wilson G, Wibault P, Janot F, Bosq J, Armand JP, et al. Rapid tumor cell proliferation after induction chemotherapy in oropharyngeal cancer. Laryngoscope. 1994;104:468–72.
36. Davis AJ, Tannock JF. Repopulation of tumour cells between cycles of chemotherapy: a neglected factor. Lancet Oncol. 2000;1:86–93.
37. Kim JJ, Tannock IF. Repopulation of cancer cells during therapy: an important cause of treatment failure. Nat Rev Cancer. 2005;5:516–25.
38. Okazaki N, Yoshino M, Yoshida T, Suzuki M, Moriyama N, Takayasu K, et al. Evaluation of the prognosis for small hepatocellular carcinoma based on tumor volume doubling time. A preliminary report. Cancer. 1989;63:2207–10.

UICC
global cancer control

IJC
International Journal of Cancer

3-Deazaneplanocin A is a promising therapeutic agent for the eradication of tumor-initiating hepatocellular carcinoma cells

Tetsuhiro Chiba[1,2]*, Eiichiro Suzuki[1,2]*, Masamitsu Negishi[2], Atsunori Saraya[2], Satoru Miyagi[2], Takaaki Konuma[2], Satomi Tanaka[2], Motohisa Tada[1], Fumihiko Kanai[1], Fumio Imazeki[1], Atsushi Iwama[2,3] and Osamu Yokosuka[1]

[1] Department of Medicine and Clinical Oncology, Graduate School of Medicine, Chiba University, 1-8-1 Inohana, Chuo-ku, Chiba 260-8670, Japan
[2] Department of Cellular and Molecular Medicine, Graduate School of Medicine, Chiba University, 1-8-1 Inohana, Chuo-ku, Chiba 260-8670, Japan
[3] JST, CREST, Sanbancho, Chiyoda-ku, Tokyo 102-0075, Japan

Recent advances in stem cell biology have identified tumor-initiating cells (TICs) in a variety of cancers including hepatocellular carcinoma (HCC). Polycomb group gene products such as BMI1 and EZH2 have been characterized as general self-renewal regulators in a wide range of normal stem cells and TICs. We previously reported that Ezh2 tightly regulates the self-renewal and differentiation of murine hepatic stem/progenitor cells. However, the role of EZH2 in tumor-initiating HCC cells remains unclear. In this study, we conducted loss-of-function assay of EZH2 using short-hairpin RNA and pharmacological inhibition of EZH2 by an S-adenosylhomocysteine hydrolase inhibitor, 3-deazaneplanocin A (DZNep). Both *EZH2*-knockdown and DZNep treatment impaired cell growth and anchorage-independent sphere formation of HCC cells in culture. Flow cytometric analyses revealed that the two approaches decreased the number of epithelial cell adhesion molecule (EpCAM)$^+$ tumor-initiating cells. Administration of 5-fluorouracil (5-FU) or DZNep suppressed the tumors by implanted HCC cells in non-obese diabetic/severe combined immunodeficient mice. Of note, however, DZNep but not 5-FU predominantly reduced the number of EpCAM$^+$ cells and diminished the self-renewal capability of these cells as judged by sphere formation assays. Our findings reveal that tumor-initiating HCC cells are highly dependent on EZH2 for their tumorigenic activity. Although further analyses of TICs from primary HCC would be necessary, pharmacological interference with EZH2 might be a promising therapeutic approach to targeting tumor-initiating HCC cells.

Cancer Cell Biology

Although first proposed approximately 50 years ago, the concept of cancer stem cells (CSCs) has drawn renewed attention from many oncologists in recent years.[1] According to the concept, tumors consist of a minor component of tumorigenic cells and a major component of non-tumorigenic cells.[2] The minor population, termed CSCs or tumor-initiating cells (TICs), organize a cellular hierarchy in a similar fashion to normal stem cell systems and exhibit pronounced tumorigenic activity in xenograft transplantation.[3,4] Recent progress in stem cell biology and technologies has facilitated the identification of TICs in a variety of cancers.[5] We previously applied side population (SP) analysis and cell sorting to

Key words: hepatocellular carcinoma, cancer stem cell, tumor-initiating cell, EZH2, DZNep

Abbreviations: 5-aza-dC: 5-aza-2′-deoxycytidine; 5-FU: 5-fluorouracil; AFP: α-fetoprotein; ALB: albumin; APC: allophycocyanin; APOC3: apolipoprotein C3; CASP3: active caspase-3; CSC: cancer stem cell; CYP1A2: cytochrome P450: subfamily 1: polypeptode 2; DZNep: 3-deazaneplanocin A; EGFP: enhanced green fluorescent protein; EpCAM: epithelial cell adhesion molecule; H3K27: histone H3 at lysine27; HCC: hepatocellular carcinoma; HMT: histone methyltransferase; Luc: luciferase; MACS: magnetic activated cell sorting; NOD/SCID: non-obese diabetic/severe combined immunodeficient; PcG: polycomb group; PEPCK: phosphoenolpyruvate carboxykinase; PRC: polycomb repressive complex; RT-PCR: reverse transcription-polymerase chain reaction; shRNA: short hairpin RNA; SP: side population; TIC: tumor-initiating cell.

Additional Supporting Information may be found in the online version of this article.

*T.C. and E.S. contributed equally to this work.

Grant sponsors: Global COE Program (Global Center for Education and Research in Immune System Regulation and Treatment), The Ministry of Education, Culture, Sports, Science and Technology, Japan, Core Research for Evolutional Science and Technology (CREST) of Japan Science and Technology Corporation (JST), The Nakayama Cancer Research Institute, The Foundation for the Promotion of Cancer Research

DOI: 10.1002/ijc.26264

History: Received 28 Jan 2011; Accepted 7 Jun 2011; Online 29 Jun 2011

Correspondence to: Atsushi Iwama, Department of Cellular and Molecular Medicine, Graduate School of Medicine, Chiba University, 1-8-1 Inohana, Chuo ward, Chiba 260-8670, Japan, Tel.: +81-43-2262189, Fax: +[81-43-2262191], E-mail: aiwama@faculty.chiba-u.jp; or Osamu Yokosuka, Department of Medicine and Clinical Oncology, Graduate School of Medicine, Chiba University, 1-8-1 Inohana, Chuo ward, Chiba 260-8670, Japan, Tel.: +81-43-2262083, Fax: +[81-43-2262088], E-mail: yokosukao@faculty.chiba-u.jp

hepatocellular carcinoma (HCC) cell lines and successfully demonstrated that SP cells in HCC showed TIC-like properties both in culture and in an *in vivo* transplant model.[6] Several surface molecules such as epithelial cell adhesion molecule (EpCAM), CD133, CD90, and CD13 have been reported as specific markers of TICs in HCC cells, although little is known about the molecular machinery operating in these cells.[7–10] Accumulating evidence suggests that TICs could play a crucial role, not only in the development, but also in the recurrence of cancer, in part due to the resistance of TICs to anti-cancer therapy.[11,12] Therefore, understanding the molecular machinery operating in TICs is indispensable both for understanding the mechanism of carcinogenesis and for the establishment of novel therapies aimed at the eradication of these cells.

It seems likely that both normal and cancer stem cells share not only a number of surface marker phenotypes but also a variety of molecular mechanisms for self-renewal and differentiation. We and others previously reported that the polycomb-group (PcG) gene product Bmi1 plays a critical role in the self-renewal of a range of somatic stem cells including hepatic stem cells.[13,14] Of note, BMI1 is required for the maintenance of not only leukemic stem cells[15] but also cancer stem cells in solid cancers such as HCC.[16] PcG complexes are key regulators of epigenetic cellular memory. They establish and maintain cellular identities during embryogenesis, development, and tumorigenesis.[17] They have also been implicated in the maintenance of embryonic and somatic stem cells.[18] Biochemical and genetic studies have demonstrated that PcG complexes can be functionally separated into at least two distinct complexes; an initiation complex, polycomb repressive complex (PRC) 2, and a maintenance complex, PRC1. Human PRC2 contains three core components: EZH2, EED, and SUZ12. PRC2 possesses catalytic activity specific for trimethylation of histone H3 at lysine 27 (H3K27). In contrast, PRC1 contains four core components; RING1, BMI1, HPH, and CBX, and possesses E3 ubiquitin ligase activity that monoubiquitylates histone H2A at lysine 119. Recently, we demonstrated that loss of Ezh2 function severely impairs the self-renewal capacity of murine hepatic stem/progenitor cells and simultaneously promotes their differentiation towards the hepatocyte lineage.[19] However, the role of EZH2 in tumor-initiating HCC cells remains unclear.

In this study, we conducted lentivirus-mediated knockdown of *EZH2* and pharmacological disruption of EZH2 to evaluate the role of EZH2 in the maintenance of TICs in HCC. We further examined whether EZH2 depletion could contribute to the eradication of the tumor-initiating HCC cells using sphere culture assays and xenograft transplantation experiments.

Material and Methods

Mice

Nonobese diabetic/severe combined immunodeficient (NOD/SCID) mice (Sankyo Laboratory Co. Ltd., Tsukuba, Japan) were bred and maintained in accordance with our institutional guidelines for the use of laboratory animals.

Cell culture and reagents

The human hepatocellular carcinoma cell lines Huh1 and Huh7 were obtained from the Health Science Research Resources Bank (HSRRB, Osaka, Japan). Cells were cultured in Dulbecco's modified Eagle's medium (Invitrogen Life Technologies, Carlsbad, CA) containing 10% FCS and 1% penicillin/streptomycin (Invitrogen). For the sphere formation assay, 1,000 cells were plated onto ultra low attachment six-well plates (Corning, Corning, NY). The number of spheres (>100 μm in diameter) was counted on day 14 of culture. For the secondary sphere formation, a single cell suspension derived from original colonies was obtained using a Neurocult chemical dissociation kit (StemCell Technologies, Vancouver, BC). For the pharmacological disruption of EZH2, 3-deazaneplanocin A (DZNep) was chemically synthesized by Chemgenesis Inc. (Tokyo, Japan). Cells were treated with DZNep (1 or 10 μM) or 5-fluorouracil (5-FU) (1 or 10 μM; Sigma-Aldrich, St Louis, MO). Likewise, the cells were treated with a G9a histone methyltransferase (HMT) inhibitor BIX01294 (1 or 10 μM) (Sigma).

Viral production and transduction

Lentiviral vectors (CS-H1-shRNA-EF-1α-EGFP) expressing short hairpin RNA (shRNA) that targets human *EZH2* (target sequence: sh-*EZH2*-1, 5′-GGAAAGAACGGAAATCTTA-3′; sh-*EZH2*-2, 5′-GGATAGAGAATGTGGGTTT-3′) and *luciferase* (*Luc*) were constructed. Flag-tagged mouse *Ezh2* cDNA was cloned into a site upstream of IRES-enhanced green fluorescent protein (EGFP) in the pMCs-IG retroviral vector. Recombinant lentiviruses and retroviruses were produced as described elsewhere.[13,14]

Cell sorting and analysis

Single-cell suspensions were stained with allophycocyanin (APC)-conjugated anti-EpCAM antibody (Biolegend, San Diego, CA) or APC-conjugated anti-CD133/1 antibody (Miltenyi Biotec, Auburn, CA). After the incubation, 1 μg/ml of propidium iodide was added to eliminate dead cells. Flow cytometirc cell sorting and analyses were performed using FACSAria (BD Biosciences, San Jose, CA). For the transplantation assay, $EpCAM^+$ cells and $CD133^+$ cells were purified with magnetic activated cell sorting (MACS) columns (Miltenyi Biotech).

Xenograft transplantation using NOD/SCID mice

A total of 2×10^6 $EpCAM^+$ or $CD133^+$ Huh7 cells stably expressing shRNA against *EZH2* or *luciferase* were suspended in DMEM and Matrigel (BD) (1:1). The *EZH2* knockdown and control cells were implanted into the subcutaneous space on the right and left sides of the backs of recipient NOD/SCID mice, respectively. In the DZNep or 5-FU treatment model, a total of 2×10^6 Huh7 cells were implanted into the subcutaneous space of the backs of NOD/SCID mice. DZNep (1 or 5 mg/Kg) and 5-FU (50 or 100 mg/Kg) was administered intraperitoneally twice per week and every 2 weeks, respectively. Tumor formation and growth were observed

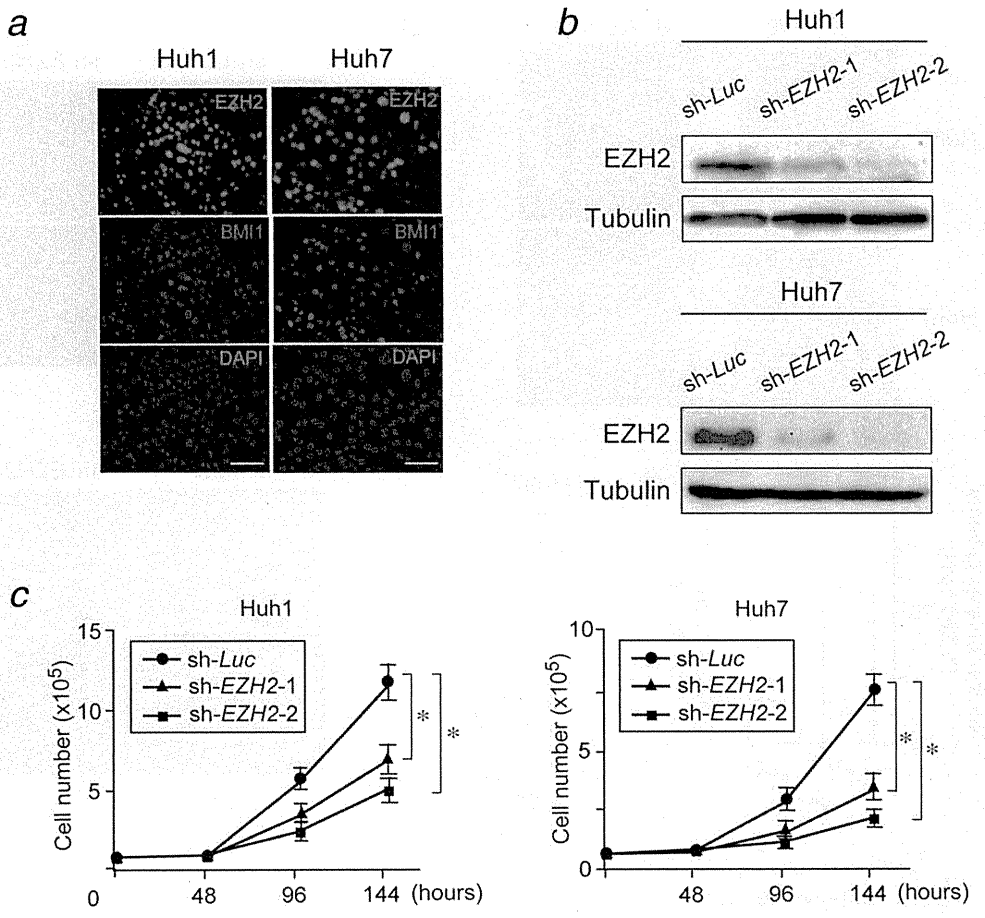

Figure 1. Basal expression and knockdown of *EZH2* in HCC cells. (*a*) Immunocytochemical analyses of EZH2 (green) and BMI1 (red) expression in Huh1 and Huh7 cells. Nuclear DAPI staining (blue) is also shown. Scale bar = 200 μm. (*b*) Cells transduced with indicated lentiviruses were selected by cell sorting for EGFP expression, and subjected to Western blot analysis using anti-EZH2 and anti-tubulin (loading control) antibodies. (*c*) Inhibition of proliferation in *EZH2* knockdown HCC cells. *Statistically significant ($p < 0.05$).

weekly. For the analyses of xenograft tumors, subcutaneous tumors were removed and minced in sterile PBS on ice. The small pieces of tumors were put in DMEM containing 5 mg/ml collagenase type II (Roche) and digested. The cell suspension was centrifuged on Ficoll (IBL, Gunma, Japan) to remove dead cells and debris. Harvested cells were subjected to flow cytometric analyses and sphere formation assays. These experiments were performed in accordance with the institutional guidelines for the use of laboratory animals.

Statistical analysis

Data are presented as the mean ± SEM. Statistical differences between 2 groups were analyzed using the Mann-Whitney U test. p values less than 0.05 were considered significant.

Results

Stable knockdown of *EZH2* in HCC cells

To investigate the role of EZH2 in HCC cells, we first examined the basal expression of EZH2 in the Huh1 and Huh7 HCC cell lines. Immunocytochemical analyses demonstrated that EZH2, as well as the PRC1 protein BMI1, were highly expressed in the nuclei of both cell lines (Fig. 1*a*). We next conducted loss-of-function analyses of EZH2 *in vitro*. We achieved the stable knockdown of *EZH2* in Huh1 and Huh7 cells with lentivirus-mediated shRNA against *EZH2* using EGFP as a marker for infection. A lentiviral vector expressing shRNA against *luciferase* was used as a control. Two different shRNAs, sh-*EZH2*-1 and sh-*EZH2*-2, both markedly repressed EZH2 protein expression and inhibited the growth of both cell lines (Fig. 1*b* and 1*c*). Because knockdown of *EZH2* and growth inhibition were more prominent with sh-*EZH2*-2 than with sh-*EZH2*-1, we used sh-*EZH2*-2 for most of the subsequent experiments. Apoptotic cell death, assessed using an anti-CASP3 antibody, was increased by *EZH2* knockdown in Huh1 and Huh7 cells approximately fourfold compared to the corresponding control cells (Supporting Information Fig. 1).

Reduced tumorigenic activity in *EZH2*-knockdown HCC cells

To examine whether *EZH2* knockdown affects the tumorigenic ability of HCC cells, we conducted a soft agar colony formation

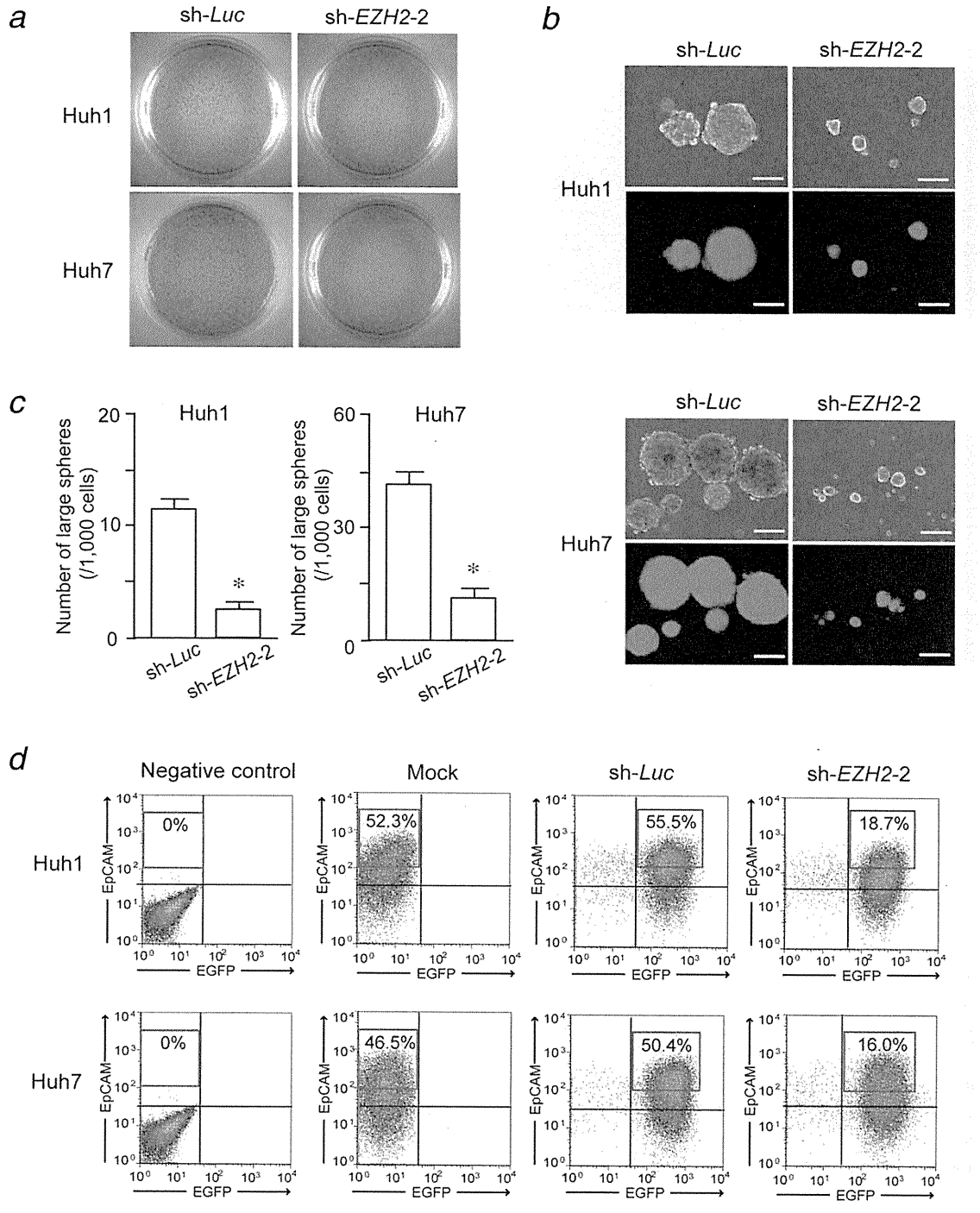

Figure 2. *In vitro* assays of HCC cells with sh-*EZH2*-2-induced *EZH2* knockdown. (*a*) Soft agar colony formation at day 21 of culture. (*b*) Non-adherent sphere formation assay at day 14 of culture. Bright-field (upper panels) and fluorescence (lower panels) images are shown. Scale bar = 100 μm. (*c*) Number of large spheres generated from 1,000 HCC cells transduced with indicated viruses. *Statistically significant ($p < 0.05$). (*d*) Flow cytometric analysis of *EZH2*-knockdown HCC cells. Flow cytometric profiles in Huh1 and Huh7 cells after the stable knockdown of *EZH2*. The percentages of EpCAM^{high} fraction are shown as the mean values for three independent analyses.

assay. Reduced colony formation was clearly observed in both cell lines following *EZH2* knockdown (Fig. 2*a*). In addition, we performed a non-adherent sphere assay, a standard assay for evaluating the stem cell activity of both normal stem cells and CSCs. Consistent with the results of the soft agar assay, sphere-forming capacity was significantly impaired in *EZH2* knockdown cells compared to the control cells (Fig. 2*b* and 2*c*). It has been documented that EpCAM^{+} cells and CD133^{+}cells

function as TICs in HCC cells, including Huh1 and Huh7 cells.[7,8] We then examined the expression of EpCAM in view of EZH2 expression using flow cytometry. Knockdown of *EZH2* decreased the EpCAM^{high} fraction from 55.5% to 18.7% in Huh1 cells and from 50.4% to 16.0% in Huh7 cells (Fig. 2*d*). Likewise, knockdown of *EZH2* in Huh7 cells decreased the CD133^{high} fraction from 40.8% to 14.3% (Supporting Information Fig. 2). In clear contrast, overexpression of *Ezh2* promoted both cell growth and sphere formation in Huh7 cells moderately but significantly (Supporting Information Fig. 3*a*–3*d*). Correspondingly, flow cytometric analyses showed an increase in the EpCAM^{high} and CD133^{high} fractions (Supporting Information Fig. 3*e*). Together, these results indicate that EZH2 expression is strongly associated with the frequency of tumor-initiating HCC cells.

Impact of EZH2 depletion on tumor-initiating HCC cells

To confirm that EZH2 directly regulates a tumorigenic subpopulation, we purified the EpCAM^{+} tumor-initiating fraction from Huh1 and Huh7 cells by flow cytometry and conducted a non-adherent sphere assay. The sphere-forming ability of EpCAM^{+} cells was significantly impaired by *EZH2* knockdown compared to that of the control cells (Supporting Information Fig. 4*a*). The secondary sphere number was also decreased by *EZH2* knockdown, indicating that EZH2 plays an important role in the maintenance of self-renewal capability in TICs (Supporting Information Fig. 4*b*). Real-time reverse transcription-polymerase chain reaction (RT-PCR) analyses of purified EpCAM^{+} Huh1 and Huh7 cells demonstrated that *EZH2* knockdown induced the down-regulation of *α-fetoprotein (AFP)*, a marker of the immature phase of hepatocytes. In clear contrast, various differentiation markers such as albumin (*ALB*) and cytochrome P450, subfamily 1, polypeptode 2 (*CYP1A2*), lipid metabolizing enzymes such as apolipoprotein C3 (*APOC3*), and enzymes involved in gluconeogenesis such as phosphoenolpyruvate carboxykinase (*PEPCK*) were upregulated to varying extents (Supporting Information Fig. 4*c*).

We next performed xenograft transplantations of sh-*EZH2*-2-expressing EpCAM^{+} cells using NOD/SCID mice (Supporting Information Fig. 4*d*). Prior to transplantation, the cells were purified by magnetic cell sorting and purity (>90%) was confirmed by flow cytometric analyses of EpCAM expression (data not shown). Importantly, and as expected, the implantation of 2×10^6 *EZH2*-knockdown EpCAM^{+} cells resulted in delayed tumor development and slower tumor growth compared with sh-*Luc* expressing control cells (Supporting Information Fig. 4*e*). Taken together, these results imply that EZH2 depletion impairs the tumorigenicity of tumor-initiating HCC cells partially through the activation of differentiation programs.

Inhibited H3K27 trymethylation by *EZH2* knockdown and DZNep treatment

Ezh2 is a histone methyltransferase and catalyzes the addition of methyl groups to H3K27. A S-adenosylhomocysteine hydrolase inhibitor, DZNep, has been reported to inhibit S-adenosylhomocysteine hydrolase and cause the retention of S-adenosylhomocysteine, thereby inhibiting S-adenosyl-L-methionine-dependent methyltransferases including EZH2. Although DZNep is not a specific inhibitor targeting EZH2, it efficiently inhibits EZH2 function.[20] DZNep also reportedly depletes EZH2 protein.[21] To examine H3K27me3 levels in *EZH2*-knockdown or DZNep-treated HCC cells, the cells were subjected to Western blotting. As expected, *EZH2* knockdown resulted in reduced levels of H3K27me3 in both HCC cells (Fig. 3*a*). Similarly, DZNep-treated HCC cells showed a significant reduction in levels of EZH2 and H3K27me3 (Fig. 3*b*).

DZNep inhibits growth and sphere formation of HCC cells

We first examined the effect of 5-FU, a widely used anti-cancer agent, on HCC cells. 5-FU efficiently inhibited the growth of HCC cells in a dose-dependent manner (Supporting Information Fig. 5*a*). Nonetheless, the effect of 5-FU to suppress non-adherent sphere formation was relatively mild compared with its effect on cell growth (Supporting Information Fig. 5*b*). Importantly, 5-FU treatment rather increased the EpCAM^{high} fraction in both Huh1 (55.9 to 83.5%) and Huh7 (45.3 to 79.1%) cells (Supporting Information Fig. 5*c*). Likewise, Huh7 cells treated with 5-FU showed an increase in the proportion of the CD133^{high} fraction from 39.0 to 85.4% (Supporting Information Fig. 6*a*). These findings indicate that tumor-initiating HCC cells were resistant to 5-FU and greatly enriched after 5-FU treatment.

Next, we examined the effect of DZNep on HCC cells *in vitro* assays. DZNep treatment inhibited growth and non-adherent sphere formation in both cell lines in a dose-dependent manner (Fig. 4*a* and 4*b*). Flow cytometric analyses revealed that the DZNep (10 μM) treatment efficiently decreased the EpCAM^{high} fraction from 49.0% to 12.5% in Huh1 cells and from 44.4% to 11.6% in Huh7 cells (Fig. 4*c*). Likewise, the CD133^{high} fraction in Huh7 cells decreased from 37.2% to 9.4% after DZNep (10 μM) treatment (Supporting Information Fig. 6*b*). These results highlighted that the biological effect of DZNep is quite different from that of 5-FU.

It has been shown that BIX01294 selectively inhibits G9a HMT activity and the generation of di-methylated H3K9.[22] To examine whether G9a inhibitor exhibits similar effect to DZNep, we conducted *in vitro* assays of Huh7 cells treated with BIX01294. Although basal level of H3K9me2/3 was comparatively high in Huh7 cells, BIX01294 treatment apparently reduced the level of H3K9me2 but not H3K9me3 (Supporting Information Fig. 7*a* and 7*b*). BIX01294 inhibited the growth and sphere formation in a dose-dependent manner (Supporting Information Fig. 7*c* and 7d). Flow cytometric analyses showed that the BIX01294 (10 μM) treatment efficiently decreased the EpCAM^{high} fraction as well as the CD133^{high} fraction in Huh7 cells (Supporting Information

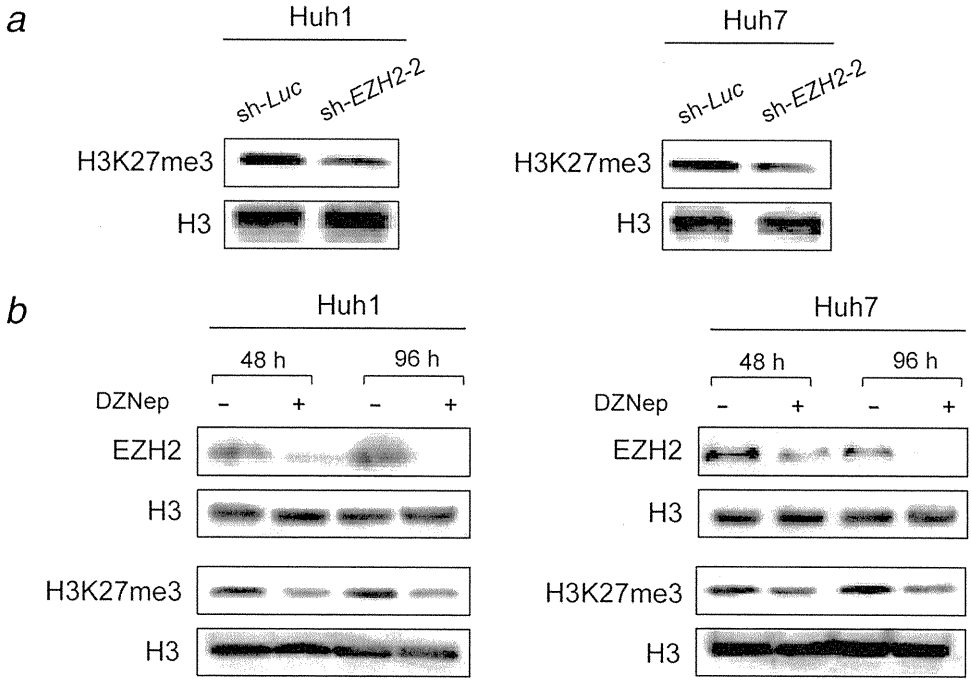

Figure 3. Changes in the trimethylated H3K27 level after EZH2 depletion. (*a*) *EZH2*-knockdown cells were subjected to Western blot analysis using anti-H3K27 and anti-H3 (loading control) antibodies. (*b*) Cells treated with DZNep (10 μM) for 48 or 96 hr were subjected to Western blot analysis using anti-EZH2, anti- trimethylated H3K27, and anti-H3 antibodies.

Fig. 7*e*). Together, depletion of H3K9me2 by BIX01294 might exert biological effects similar to DZNep.

Effect of DZNep on tumor-initiating Huh7 cells

To evaluate directly the action of DZNep towards TICs, we purified EpCAM$^+$ cells from Huh7 cells by cell sorting and conducted sphere formation assays. DZNep markedly impaired primary sphere formation and even more severely impaired secondary sphere formation (Fig. 5*a* and 5*b*). These results indicate that DZNep inhibits self-renewal of tumor-initiating HCC cells. The immunostaining of CASP-3 showed that DZNep treatment induced apoptotis dose-dependently (Fig. 5*c*). The percentage of apoptotic cells among EpCAM$^+$ Huh7 cells treated with DZNep (10 μM) was approximately eight-fold higher than among control cells (Fig. 5*d*).

Subsequently, we determined the ability of DZNep to eradicate TICs using xenograft NOD/SCID mouse models. After the implantation of 2×10^6 Huh7 cells into NOD/SCID mice, and either 5-FU (every 2 weeks) or DZNep (twice a week) was administered intraperitoneally to recipient mice. Tumor initiation and growth were apparently suppressed by both 5-FU and DZNep treatment in a dose-dependent manner. However, DZNep was more effective than 5-FU (Fig. 6*a* and *b*). Flow cytometric analyses of xenograft tumors showed that 5-FU treatment subsequently enriched tumor-initiating EpCAM^{high} cells as observed in *in vitro* analyses (Fig. 6*c*). In clear contrast, DZNep administration resulted in a drastic decrease in tumor-initiating EpCAM^{high} cells (Fig. 6*c*). We next purified EpCAM$^+$ cells derived from xenograft tumors and performed sphere formation assays. EpCAM$^+$ cells treated with DZNep gave rise to significantly fewer spheres in both primary and secondary cultures than those treated with 5-FU (Supporting Information Fig. 8*a* and 8*b*).

Together, these results indicate that DZNep suppresses tumor growth by directly affecting the growth and self-renewal of TICs.

Discussion

Accumulating evidence implies that the overexpression of EZH2 and deregulation of H3K27 methylation play an important role in a variety of cancers.[23] For example, *EZH2* expression is highly upregulated in prostate cancer, and frequent genomic loss of *microRNA-101* targeting the *EZH2* mRNA has been proposed as one mechanism responsible for the upregulation.[24] We and others reported that the level of EZH2 expression is closely associated with the progression and prognosis of HCC.[25,26] All of these findings highlight the importance of EZH2 in hepatocarcinogenesis and implicate EZH2 in regulation of the self-renewal capacity of tumor-initiating HCC cells.

In this study, we first conducted the loss-of-function assays in non-purified Huh1 and Huh7 cells. Lentiviral knockdown of *EZH2* significantly reduced both anchorage-independent colony formation and sphere formation by Huh1 and Huh7 cells in culture. Importantly, flow cytometric analysis showed a significant decrease in the percentage of

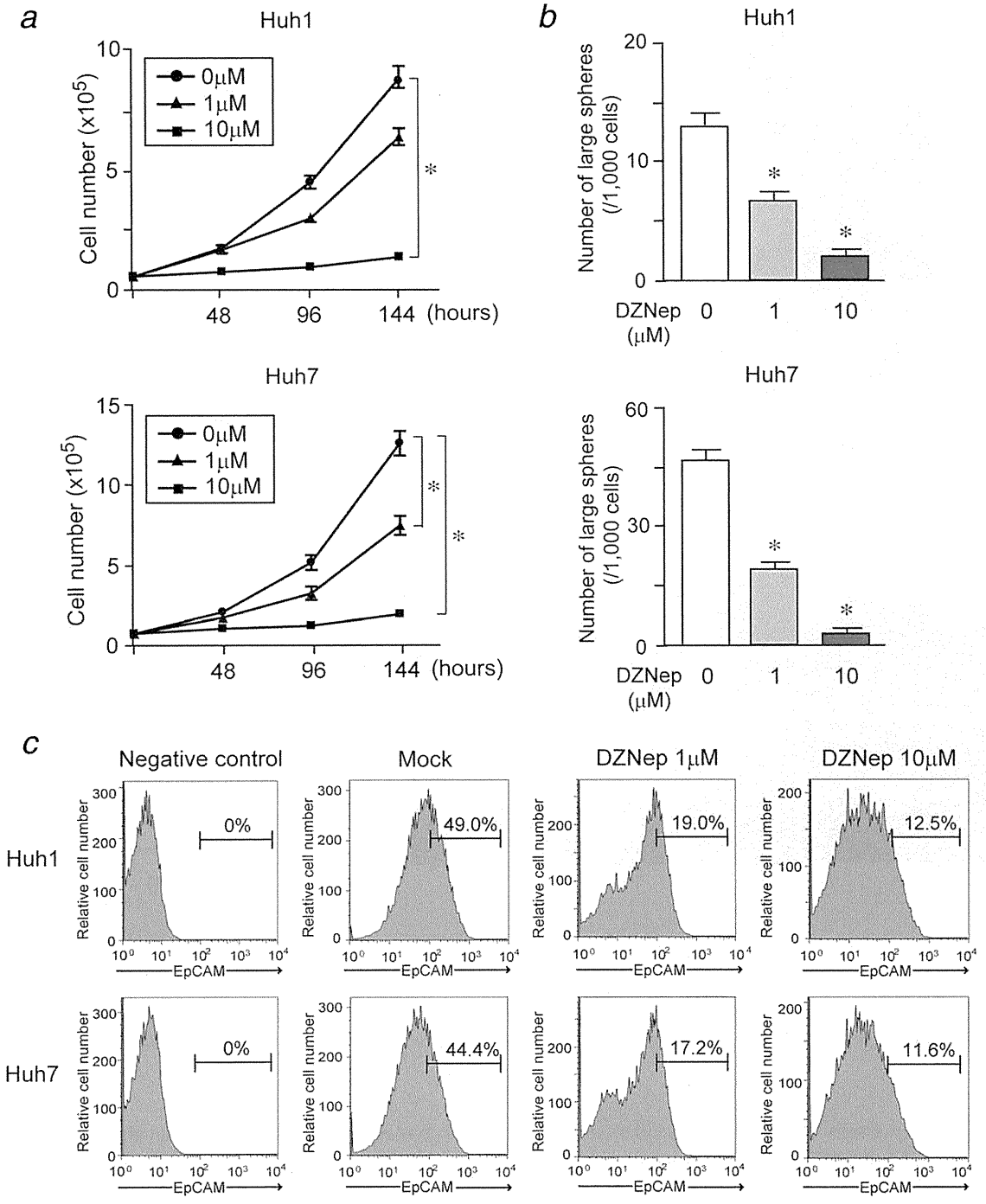

Figure 4. *In vitro* assays of HCC cells treated with DZNep. (*a*) Dose-dependent inhibition of proliferation in DZNep-treated HCC cells. *Statistically significant ($p < 0.05$). (*b*) Number of large spheres generated from 1,000 HCC cells at day 14 of culture. *Statistically significant ($p < 0.05$). (*c*) Flow cytometric profiles of HCC cells treated with DZNep (1 or 10 μM) for 144 hr. The percentages of $EpCAM^{high}$ fraction are shown as the mean values for three independent analyses.

$EpCAM^{high}$ cells following *EZH2* knockdown. Furthermore, $EpCAM^{+}$ cells purified from Huh1 and Huh7 cells exhibited reduced tumorigenicity in a xenograft transplantation assay when EZH2 was depleted. In clear contrast with the knockdown assays, overexpression of *Ezh2* in Huh7 cells enhanced their sphere forming ability and increased the number of $EpCAM^{high}$ and $CD133^{high}$ cells. These results implicated that EZH2 directly regulates a tumor-initiating subpopulation.

Of interest, *EZH2* knockdown cells also showed reduced expression of AFP, a hepatic stem/progenitor cell marker,

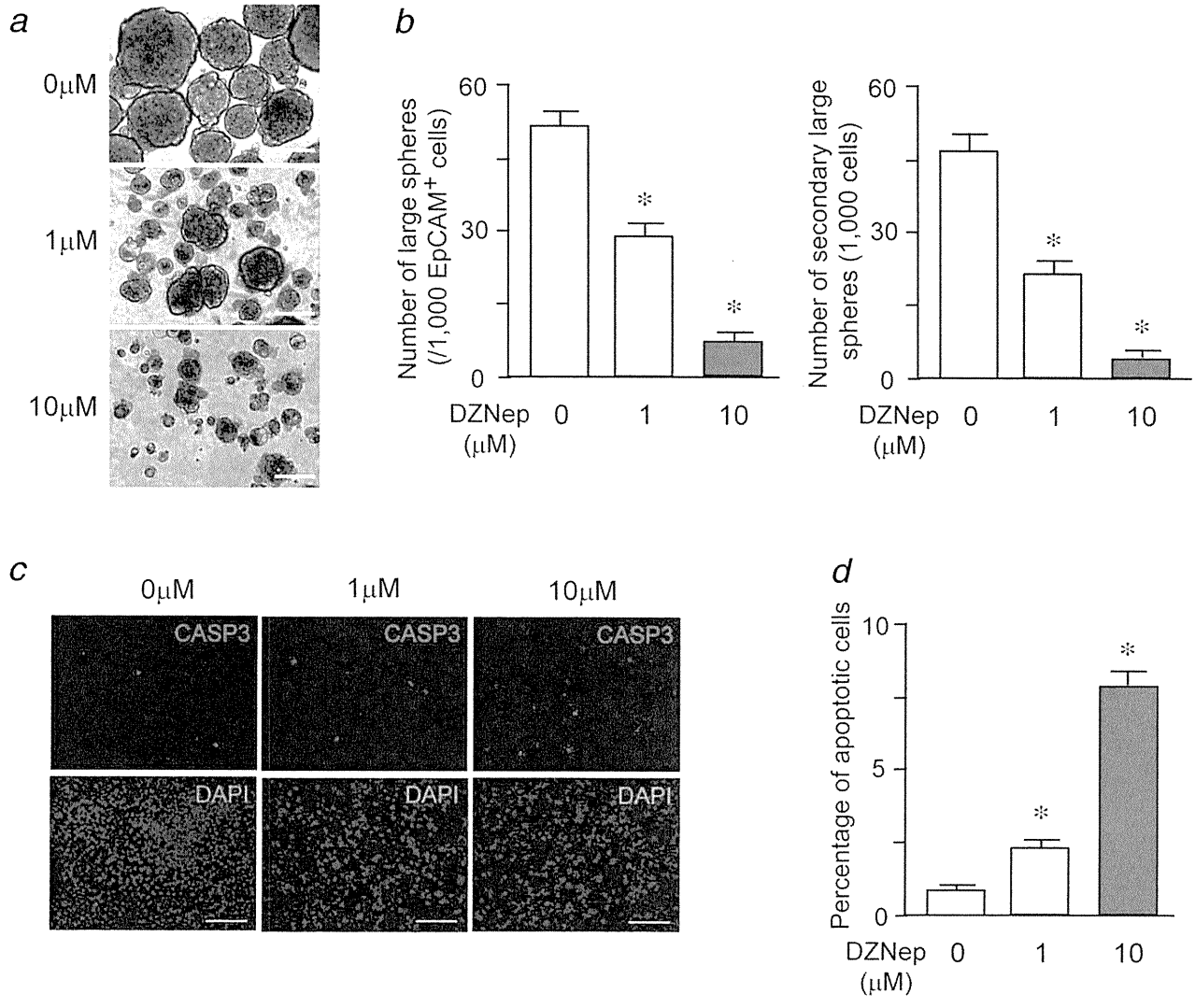

Figure 5. Effect of DZNep in tumor-initiating EpCAM$^+$ cells. (*a*) Bright-field images of non-adherent spheres on day 14 of culture. Scale bar = 100 μm. (*b*) Number of original spheres generated from 1,000 EpCAM$^+$ cells at day 14 of culture and secondary spheres 14 days after replating. *Statistically significant ($p < 0.05$). (*c*) Detection of apoptotic cell death by immunostaining of active caspase-3 (CASP3). Scale bar = 200 μm. (*d*) Quantification of the percentage of apoptotic cells is indicated at the right. *Statistically significant ($p < 0.05$).

and enhanced expression of various differentiation markers of hepatocytes. Analysis of transgenic mice in which Myc expression could be conditionally regulated revealed that multiple HCCs induced by overexpression of Myc lose their neoplastic properties and differentiate into hepatocytes and cholangiocytes upon inactivation of Myc, followed by a reduction in tumor volume and prolonged survival of the hosts.[27] Overexpression of hepatocyte nuclear factor 4α, a well-known liver-enriched transcription factor, reportedly impairs the tumorigenic activity of HCC cells by promoting their differentiation.[28] Given that the tumorigenicity of TICs is closely associated with their immature state in terms of differentiation, the induction of differentiation programs in TICs is a promising approach for targeting TICs.[29,30]

It has recently been reported that the S-adenosylhomocysteine hydrolase inhibitor DZNep depletes cellular levels of PRC2 components including EZH2, SUZ12, and EED and selectively inhibits the trimethylation of H3K27.[21] Intriguingly, DZNep more effectively induces apoptosis in transformed cells than normal cells.[21] Moreover, DZNep treatment has been demonstrated to be effective in abrogating the self-renewal and tumorigenicity of glioblastoma TICs at levels comparative to *EZH2* knockdown.[31]

As expected, our results showed that HCC cells treated with DZNep showed reduced levels of EZH2 and trimethylated H3K27. To elucidate whether DZNep has an inhibitory effect on tumor-initiating HCC cells, we performed *in vitro* assays and xenograft transplantation assays. Sphere formation

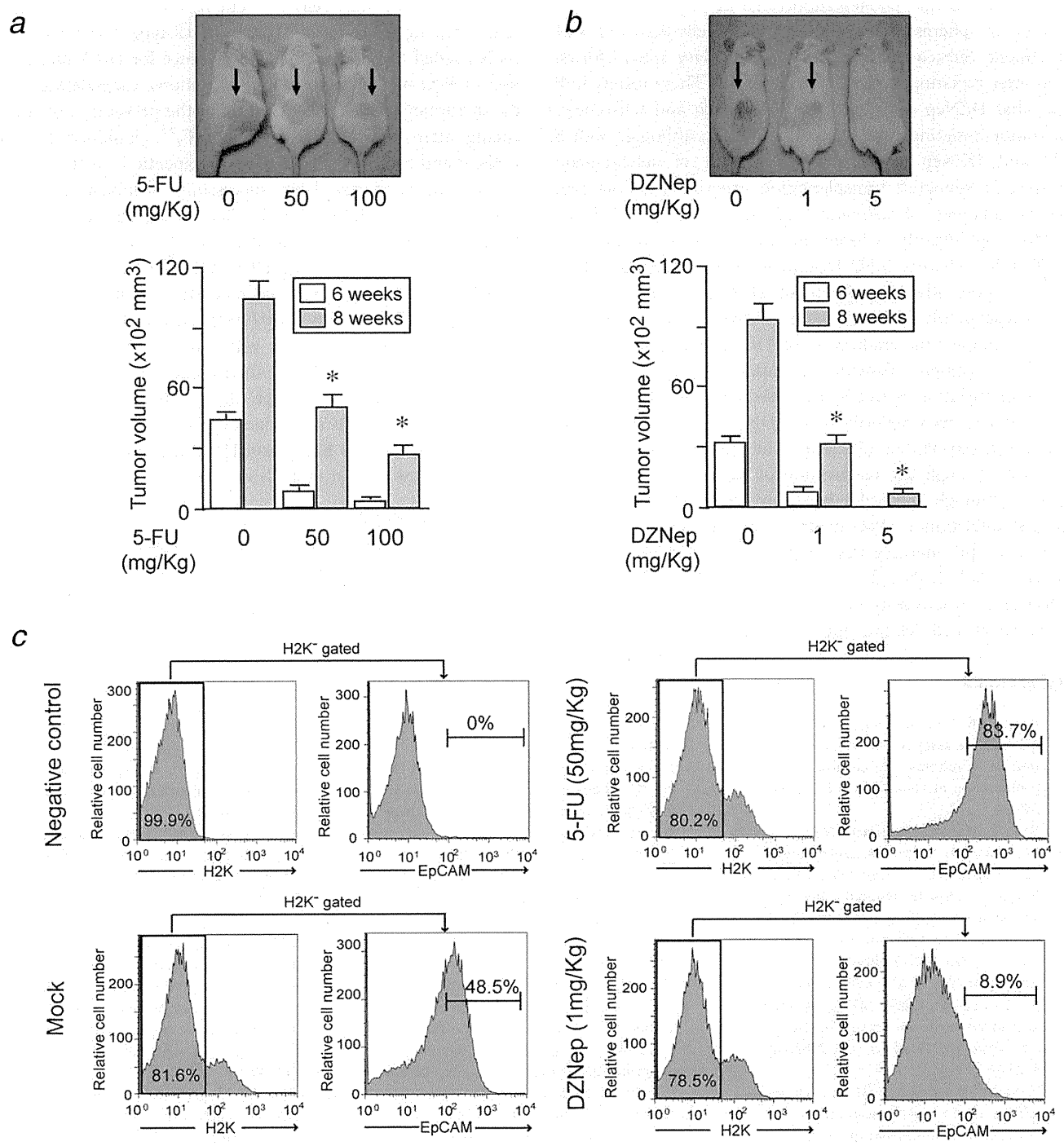

Figure 6. Transplantation and reanalysis of xenograft tumors. (*a*) A total of 2×10^6 Huh7 cells were transplanted into the subcutaneous space of NOD/SCID mice. Growth of subcutaneous tumors (arrows) was apparently suppressed by 5-FU treatment in a dose-dependent manner 6 weeks after transplantation (left panel). Subcutaneous tumor volume was determined at 6 and 8 weeks after transplantation (right panel). *Statistically significant ($p < 0.05$). (*b*) A total of 2×10^6 Huh7 cells were transplanted into NOD/SCID mice. Tumor growth (arrows) was obviously suppressed by DZNep in a dose-dependent manner 6 weeks after the transplantation (left panel). Tumor volume was determined at 6 and 8 weeks after transplantation (right panel). *Statistically significant ($p < 0.05$). (*c*) Flow cytometric profiles of xenograft tumor cells treated with 5-FU or DZNep. The expression of EpCAM was assessed in $H2K^-$ donor tumor cells. The percentages of $EpCAM^{high}$ fraction are shown as the mean values for three independent analyses. [Color figure can be viewed in the online issue, which is available at wileyonlinelibrary.com.]

assays showed that DZNep suppressed more severely the formation of spheres originated from HCC cells than did 5-FU treatment. Subsequent analyses for secondary sphere formation after replating showed similar results. These results indicate that DZNep directly affects the growth and self-renewal of tumor-initiating HCC cells. In addition, although both 5-FU and DZNep suppressed the growth of subcutaneous tumors in xenograft transplantation experiments, flow cytometric analyses of xenograft tumors clearly revealed that DZNep significantly reduced the number of tumor-initiating HCC cells, whereas 5-FU treatment inversely enriched these cells. Importantly, the effects of DZNep were augmented dose-dependently. Taken together, DZNep could be of therapeutic value for the eradication of TICs in HCC.

Transcriptional silencing of tumor suppressor genes by DNA methylation is frequently observed in a variety of cancer.[32] It has been believed that a DNA demethylating agent, 5-aza-2′-deoxycytidine (5-aza-dC), inhibits the growth of cancer cells through the reactivation of these tumor suppressor genes, although 5-aza-dC has only shown limited efficacy against solid tumors. PcG-mediated trimethylation on H3K27 reportedly pre-marks genes for *de novo* methylation in colon cancer cells.[33] Although DZNep or *EZH2* knockdown is not effective in reactivating genes silenced by DNA methylation, it reactivates developmental genes not silenced by DNA methylation in cancer cells.[20,34] The manner of gene silencing might depend on the gene locus and cell-type. Further analysis is needed to understand the preference for DNA methylation or PcG-mediated histone modifications. Considering that the disruption of EZH2 contributes to the prevention of resilencing after the removal of 5-aza-dC,[35] combined use of DZNep and 5-aza-dC might be of therapeutic benefit.

In conclusion, we have successfully demonstrated that both *EZH2* knockdown and pharmacological ablation of EZH2 significantly reduced the number and tumorigenic potential of tumor-initiating HCC cells. This effect might be attributed to the impaired self-renewal capability of tumor-initiating HCC cells caused by interference with EZH2.

However, further analysis will definitely be necessary to determine the effort of EZH2 interference in primary tumor-initiating HCC cells. Although the exploration of potential therapies targeting TICs has just begun, compounds targeting PcG proteins such as EZH2 and HMT inhibitors might be of use for the eradication of TICs in HCC.

Acknowledgement

The authors thank Dr. Kristian Helin (University of Copenhagen) for the anti-EZH2 antibody and Dr. Toshio Kitamura (Tokyo University) for the pMCs-IG retroviral vector, and Drs. Yosuke Osawa and Atsushi Suetsugu (Gifu University) and Dr. Taro Yamashita (Kanazawa University), for valuable discussions.

References

1. Bruce WR, Van Der Gaag H. A quantitative assay for the number of murine lymphoma cells capable of proliferation in vivo. *Nature* 1963;199:79–80.
2. Reya T, Morrison SJ, Clarke MF, Weissman IL. Stem cells, cancer, and cancer stem cells. *Nature* 2001;414:105–11.
3. Bonnet D, Dick JE. Human acute myeloid leukemia is organized as a hierarchy that originates from a primitive hematopoietic cell. *Nat Med* 1997;3:730–7.
4. Al-Hajj M, Wicha MS, Benito-Hernandez A, Morrison SJ, Clarke MF. Prospective identification of tumorigenic breast cancer cells. *Proc Natl Acad Sci USA* 2003;100:3983–8.
5. Visvader JE, Lindeman GJ. Cancer stem cells in solid tumours: accumulating evidence and unresolved questions. *Nat Rev Cancer* 2008;8:755–68.
6. Chiba T, Kita K, Zheng YW, Yokosuka O, Saisho H, Iwama A, Nakauchi H, Taniguchi H. Side population purified from hepatocellular carcinoma cells harbors cancer stem cell-like properties. *Hepatology* 2006;44:240–51.
7. Yamashita T, Ji J, Budhu A, Forgues M, Yang W, Wang HY, Jia H, Ye Q, Qin LX, Wauthier E, Reid LM, Minato H, et al. EpCAM-positive hepatocellular carcinoma cells are tumor-initiating cells with stem/progenitor cell features. *Gastroenterology* 2009;136:1012–24.
8. Ma S, Chan KW, Hu L, Lee TK, Wo JY, Ng IO, Zheng BJ, Guan XY. Identification and characterization of tumorigenic liver cancer stem/progenitor cells. *Gastroenterology* 2007;132:2542–56.
9. Yang ZF, Ho DW, Ng MN, Lau CK, Yu WC, Ngai P, Chu PW, Lam CT, Poon RT, Fan ST. Significance of CD90+ cancer stem cells in human liver cancer. *Cancer Cell* 2008;13:153–66.
10. Haraguchi N, Ishii H, Mimori K, Tanaka F, Ohkuma M, Kim HM, Akita H, Takiuchi D, Hatano H, Nagano H, Barnard GF, Doki Y, et al. CD13 is a therapeutic target in human liver cancer stem cells. *J Clin Invest* 2010;120:3326–39.
11. Jordan CT, Guzman ML, Noble M. Cancer stem cells. *N Engl J Med* 2006;355:1253–61.
12. Dean M, Fojo T, Bates S. Tumour stem cells and drug resistance. *Nat Rev Cancer* 2005;5:275–84.
13. Iwama A, Oguro H, Negishi M, Kato Y, Morita Y, Tsukui H, Ema H, Kamijo T, Katoh-Fukui Y, Koseki H, van Lohuizen M, Nakauchi H. Enhanced self-renewal of hematopoietic stem cells mediated by the polycomb gene product Bmi-1. *Immunity* 2004;21:843–51.
14. Chiba T, Zheng YW, Kita K, Yokosuka O, Saisho H, Onodera M, Miyoshi H, Nakano M, Zen Y, Nakanuma Y, Nakauchi H, Iwama A, et al. Enhanced self-renewal capability in hepatic stem/progenitor cells drives cancer initiation. *Gastroenterology* 2007;133:937–50.
15. Lessard J, Sauvageau G. Bmi-1 determines the proliferative capacity of normal and leukaemic stem cells. *Nature* 2003;423:255–60.
16. Chiba T, Miyagi S, Saraya A, Aoki R, Seki A, Morita Y, Yonemitsu Y, Yokosuka O, Taniguchi H, Nakauchi H, Iwama A. The polycomb gene product BMI1 contributes to the maintenance of tumor-initiating side population cells in hepatocellular carcinoma. *Cancer Res* 2008;68:7742–49.
17. Simon JA, Kingston RE. Chromatin dynamics mechanisms of polycomb gene silencing: knowns and unknowns. *Nat Rev Mol Cell Biol* 2009;10:697–708.
18. Pietersen AM, van Lohuizen M. Stem cell regulation by polycomb repressors: postponing commitment. *Curr Opin Cell Biol* 2008;20:201–7.
19. Aoki R, Chiba T, Miyagi S, Negishi M, Konuma T, Taniguchi H, Ogawa M, Yokosuka O, Iwama A. The polycomb group gene product Ezh2 regulates proliferation and differentiation of murine hepatic stem/progenitor cells. *J Hepatol* 2010;52:854–63.

20. Miranda TB, Cortez CC, Yoo CB, Liang G, Abe M, Kelly TK, Marquez VE, Jones PA. DZNep is a global histone methylation inhibitor that reactivates developmental genes not silenced by DNA methylation. *Mol Cancer Ther* 2009;8:1579–88.
21. Tan J, Yang X, Zhuang L, Jiang X, Chen W, Lee PL, Karuturi RK, Tan PB, Liu ET, Yu Q. Pharmacologic disruption of polycomb-repressive complex 2-mediated gene repression selectively induces apoptosis in cancer cells. *Genes Dev* 2007; 21:1050–63.
22. Kubicek S, O'sullivan RJ, August EM, Hickey ER, Zhang Q, Teodoro ML, Rea S, Mechtler K, Kowalski JA, Homon CA, Kelly TA, Jenuwein T. Reversal of H3K9me2 by a small-molecule inhibitor for the G9a histone methyltransferase. *Mol Cell* 2007 9;25:473–81.
23. Martinez-Garcia E, Licht JD. Deregulation of H3K27 methylation in cancer. *Nat Genet* 2010;42:100–1.
24. Varambally S, Cao Q, Mani RS, Shankar S, Wang X, Ateeq B, Laxman B, Cao X, Jing X, Ramnarayanan K, Brenner JC, Yu J, et al. Genomic loss of microRNA-101 leads to overexpression of histone methyltransferase EZH2 in cancer. *Science* 2008;322:1695–9.
25. Yonemitsu Y, Imazeki F, Chiba T, Fukai K, Nagai Y, Miyagi S, Arai M, Aoki R, Miyazaki M, Nakatani Y, Iwama A, Yokosuka O. Distinct expression of polycomb group proteins EZH2 and BMI1 in hepatocellular carcinoma. *Hum Pathol* 2009;40:1304–11.
26. Sasaki M, Ikeda H, Itatsu K, Yamaguchi J, Sawada S, Minato H, Ohta T, Nakanuma Y. The overexpression of polycomb group proteins Bmi1 and EZH2 is associated with the progression and aggressive biological behavior of hepatocellular carcinoma. *Lab Invest* 2008;88:873–82.
27. Shachaf CM, Kopelman AM, Arvanitis C, Karlsson A, Beer S, Mandl S, Bachmann MH, Borowsky AD, Ruebner B, Cardiff RD, Yang Q, Bishop JM, et al. MYC inactivation uncovers pluripotent differentiation and tumour dormancy in hepatocellular cancer. *Nature* 2004;431: 1112–17.
28. Yin C, Lin Y, Zhang X, Chen YX, Zeng X, Yue HY, Hou JL, Deng X, Zhang JP, Han ZG, Xie WF. Differentiation therapy of hepatocellular carcinoma in mice with recombinant adenovirus carrying hepatocyte nuclear factor-4alpha gene. *Hepatology* 2008;48:1528–39.
29. Chiba T, Kamiya A, Yokosuka O, Iwama A. Cancer stem cells in hepatocellular carcinoma: recent progress and perspective. *Cancer Lett* 2009;286:145–53.
30. Sell S. Stem cell origin of cancer and differentiation therapy. *Crit Rev Oncol Hematol* 2004;51:1–28.
31. Suvà ML, Riggi N, Janiszewska M, Radovanovic I, Provero P, Stehle JC, Baumer K, Le Bitoux MA, Marino D, Cironi L, Marquez VE, Clément V, et al. EZH2 is essential for glioblastoma cancer stem cell maintenance. *Cancer Res* 2009;69: 9211–18.
32. Baylin SB. DNA methylation and gene silencing in cancer. *Nat Clin Pract Oncol* 2005;2 (Suppl 1):S4–S11.
33. Schlesinger Y, Straussman R, Keshet I, Farkash S, Hecht M, Zimmerman J, Eden E, Yakhini Z, Ben-Shushan E, Reubinoff BE, Bergman Y, Simon I, et al. Polycomb-mediated methylation on Lys27 of histone H3 pre-marks genes for de novo methylation in cancer. *Nat Genet* 2007;39: 232–6.
34. Kondo Y, Shen L, Cheng AS, Ahmed S, Boumber Y, Charo C, Yamochi T, Urano T, Furukawa K, Kwabi-Addo B, Gold DL, Sekido Y, et al. Gene silencing in cancer by histone H3 lysine 27 trimethylation independent of promoter DNA methylation. *Nat Genet* 2008;40:741–50.
35. Kodach LL, Jacobs RJ, Heijmans J, van Noesel CJ, Langers AM, Verspaget HW, Hommes DW, Offerhaus GJ, van den Brink GR, Hardwick JC. The role of EZH2 and DNA methylation in the silencing of the tumour suppressor RUNX3 in colorectal cancer. *Carcinogenesis* 2010;31: 1567–75.

Research Article

EASL EUROPEAN ASSOCIATION FOR THE STUDY OF THE LIVER | JOURNAL OF HEPATOLOGY

Altered composition of fatty acids exacerbates hepatotumorigenesis during activation of the phosphatidylinositol 3-kinase pathway

Yotaro Kudo[1], Yasuo Tanaka[1], Keisuke Tateishi[1,*], Keisuke Yamamoto[1], Shinzo Yamamoto[1], Dai Mohri[1], Yoshihiro Isomura[1], Motoko Seto[1], Hayato Nakagawa[1], Yoshinari Asaoka[1], Motohisa Tada[2], Miki Ohta[1], Hideaki Ijichi[1], Yoshihiro Hirata[1], Motoyuki Otsuka[1], Tsuneo Ikenoue[1], Shin Maeda[3], Shuichiro Shiina[1], Haruhiko Yoshida[1], Osamu Nakajima[4], Fumihiko Kanai[2], Masao Omata[5], Kazuhiko Koike[1]

[1]*Department of Gastroenterology, Graduate School of Medicine, The University of Tokyo, 7-3-1 Hongo, Bunkyo-ku, Tokyo 113-8655, Japan;* [2]*Department of Medicine and Clinical Oncology, Graduate School of Medicine, Chiba University, 1-8-1 Inohana, Chuo-ku, Chiba-shi, Chiba 260-8670, Japan;* [3]*Department of Gas troenterology, Yokohama City University, Graduate School of Medicine, 3-9 Fuku-ura, Kanazawa-ku, Yokohama 236-0004, Japan;* [4]*Research Laboratory for Molecular Genetics, Yamagata University, Yamagata 990-9585, Japan;* [5]*Yamanashi Prefectural Central Hospital, 1-1-1 Fujimi, Kofu-shi, Yamanashi 400-8506, Japan*

Background & Aims: Some clinical findings have suggested that systemic metabolic disorders accelerate *in vivo* tumor progression. Deregulation of the phosphatidylinositol 3-kinase (PI3K)/Akt pathway is implicated in both metabolic dysfunction and carcinogenesis in humans; however, it remains unknown whether the altered metabolic status caused by abnormal activation of the pathway is linked to the protumorigenic effect.

Methods: We established hepatocyte-specific *Pik3ca* transgenic (Tg) mice harboring N1068fs*4 mutation.

Results: The Tg mice exhibited hepatic steatosis and tumor development. PPARγ-dependent lipogenesis was accelerated in the Tg liver, and the abnormal profile of accumulated fatty acid (FA) composition was observed in the tumors of Tg livers. In addition, the Akt/mTOR pathway was highly activated in the tumors, and in turn, the expression of tumor suppressor genes including *Pten*, *Xpo4*, and *Dlc1* decreased. Interestingly, we found that the suppression of those genes and the enhanced *in vitro* colony formation were induced in the immortalized hepatocytes by the treatment with oleic acid (OA), which is one of the FAs that accumulated in tumors.

Conclusions: Our data suggest that the unusual FA accumulation has a possible role in promoting *in vivo* hepato-tumorigenesis under constitutive activation of the PI3K pathway. The *Pik3ca* Tg mice might help to elucidate molecular mechanisms by which metabolic dysfunction contributes to *in vivo* tumor progression.

Keywords: Hepatocellular carcinoma; Fatty acids; NAFLD; Tumor suppressor genes.

Received 3 October 2010; received in revised form 25 March 2011; accepted 27 March 2011; available online 19 May 2011

*Corresponding author. Tel.: +81 3 3815 5411x33070; fax: +81 3 3814 0021.

E-mail address: ktate-tky@umin.ac.jp (K. Tateishi).

Abbreviations: PI3K, phosphatidylinositol 3-kinase; Tg, transgenic; FA, fatty acid; OA, oleic acid; HCC, hepatocellular carcinoma; PTEN, phosphatase and tensin homolog deleted on chromosome 10; FBS, fetal bovine serum; Erk, extracellular signal-regulated kinase; WT, wild type; PA, palmitic acid; H&E, hematoxylin and eosin; NASH, non-alcoholic steatohepatitis.

Introduction

Accumulating clinical evidence suggests that systemic metabolic disorders including obesity and insulin resistance can affect or even promote *in vivo* tumor progression [1–4]. Some studies have outlined the impact of fat-enriched diets in the development of hepatocellular carcinoma (HCC) [5–7]. However, the mechanistic insights regarding metabolites or cellular signaling responsible for the development of HCC in altered metabolic states remain unknown.

The phosphatidylinositol 3-kinase (PI3K)/Akt signaling pathway is involved in various cellular processes including cell metabolism, growth, and survival [8,9]. The altered expression and mutation of PI3K/Akt-related signaling components have been detected in some human cancers [10]. In particular, the *PIK3CA* gene encoding p110α, which is a catalytic subunit of PI3K, has somatic mutations in some carcinomas [11]. Additionally, a mutation in its kinase domain has been reported in HCC and gastric cancer [12]. These findings indicate that deregulated PI3K activity plays certain roles in oncogenesis in humans [11,13]. PI3K signaling is antagonized by phosphatase and tensin homolog deleted on chromosome 10 (PTEN) phosphatase [14]. The expression of PTEN is decreased or absent in approximately half of HCC patients [15], and hepatocyte-specific *Pten* knockout

mice develop steatohepatitis and HCC [16]. These findings indicate that PTEN is a tumor suppressor in the liver [17]. Although recent reports have suggested unique functions of PTEN that are independent of the PI3K-Akt axis [18–20], it is unknown whether the phenotype in *Pten*-deficient mice is due to PI3K-dependent or PI3K-independent processes.

To address the pathological consequences caused by the abnormal activation of PI3K pathway *in vivo*, we generated liver-specific *Pik3ca* transgenic (Tg) mice. In this study, we proposed that abnormal fat composition, as observed in the *Pik3ca* Tg liver, is a mechanism by which metabolic deregulation is linked to *in vivo* tumor progression.

Materials and methods

Generation of Pik3ca Tg mice

The *Pik3ca* Tg mice were generated as described previously [21]. Briefly, Myc-tagged mouse *Pik3ca* cDNA (N1068fs*4) was cloned into the p2335A-1 vector (provided by Drs. Palmiter and Chisari) [22,23]. The microinjection was conducted by the Research Laboratory for Molecular Genetics, Yamagata University. Founder BDF1 mice (F0) were backcrossed with C57BL/6JJcl mice (CLEA Japan, Japan), and F5 mice were analyzed. The primers for genotyping were 5′-ATGGAACAGAAACTCATCTCT-3′ and 5′-GGGTGACACTTACGAAAAT-3′. All procedures involving animals were performed in accordance with protocols approved by the institutional committee for animal research at the University of Tokyo and complied with the Guide for the Care and Use of Laboratory Animals.

Cell cultures, viruses, and treatment with fatty acids

Lentiviral short hairpin RNA vectors were purchased from Open Biosystems (Huntsville, AL, USA). BNL-CL2 cells were infected with the virus according to the manufacturer's protocol and selected by puromycin. BNL-CL2 cells were incubated with either 50 μmol/L fatty acids or ethanol (mock) for 12 h in the absence of fetal bovine serum (FBS) in some experiments.

Antibodies and primers

The primers for quantitative RT-PCR are shown in Supplementary Table 1. Antibodies against phospho-Akt (Ser473 and Thr308), Akt, phospho-extracellular signal-regulated kinase (Erk) 1/2 (Thr202/Tyr204), Erk1/2, phospho-TSC2, phospho-S6K, TSC2, S6K, and SREBP1 were obtained from Cell Signaling Technology (Danvers, MA, USA). The anti-PTEN antibody was purchased from Neomarkers Inc. (Frement, CA, USA). The anti-TFIID antibody was purchased from Upstate Biotechnology Inc. (Lake Placid, NY, USA). For immunohistochemistry, the anti-phospho-Akt (Ser473) antibody and anti-Myc antibodies (Cell Signaling Technology) were used. The immunoblot data were quantified using Multi Gauge ver. 3.1 software (Fuji Film Corp., Tokyo, Japan).

Triacylglycerol content, serum alanine aminotransferase (ALT) levels, and FA composition

Triacylglycerols were extracted from the liver with chloroform–methanol (2:1, v/v), and the levels were determined by the GK-GPO method (Wako, Tokyo, Japan). Serum samples for ALT measurement were collected after a 16-h starvation (SRL, Tokyo, Japan). Fatty acids were extracted from frozen liver samples, and the composition was analyzed by gas chromatography (Kotobiken Medical Laboratories, Inc., Tokyo, Japan).

Glucose tolerance tests

Glucose was intraperitoneally injected into 8-week-old mice fasting for 16 h (1.5 mg of glucose/g body weight). Glucose concentration was measured using the FreeStyle FREEDOM Blood Glucose Monitoring System (Nipro, Tokyo, Japan) at 0, 15, 30, 60, 90, and 120 min after injection.

Oxidative stress evaluation

The measurement of hydrogen peroxide concentrations was performed by the Colorimetric Hydrogen Peroxide Kit (Assay Designs, Inc., Ann Arbor, MI, USA). Thiobarbituric acid reactive substances (TBARS) were measured by the TBARS Assay Kit (ZeptoMetrix, Buffalo, NY, USA).

Immunohistochemistry

Antigen retrieval on paraffin sections was performed by the acetylation method. Proteins were visualized using the standard 3,3′-diaminobenzidine protocol.

Soft agar assay

The lower layer of 0.5% agar in media was placed in a 35-mm dish. Cells (2.5×10^4) were suspended in the upper layer of 0.3% agar. Colonies (>25 μm in diameter) were counted after 14 days. Oleic acid (OA) (50 μmol/L) or ethanol was added to the upper layer in some experiments.

Statistics

All results are indicated as means ± SE. Statistics were performed by Student's *t*-test or ANOVA followed by Fisher's PLSD host-hoc test. *p*-Values <0.05 were considered statistically significant.

Results

Generation of hepatocyte-specific Pik3ca Tg mice

We established 2 independent lines of hepatocyte-specific Tg mice (*Pik3ca* Tg mice) harboring an "N1068fs*4" mutation in the kinase domain [12]. Myc-tagged mutant *Pik3ca* was designed to be expressed under the albumin promoter (Supplementary Fig. 1), and the liver-specific expression of the transgene was confirmed as shown in Fig. 1A. To assess the *in vivo* effect of the *Pik3ca* N1068fs*4 transgene, we analyzed the activity of molecules downstream of PIK3CA including Akt, TSC2, and S6K via immunoblotting. The phosphorylation of Akt, TSC2, and S6K was clearly increased both in the two lines of Tg livers, but not in the wild-type (WT) livers (Fig. 1B).

Constitutive activation of Pik3ca leads to fat accumulation in the liver

Both lines of *Pik3ca* Tg mice survived, and no difference in total body weight was observed between *Pik3ca* Tg and WT mice at 4 or 24 weeks of age (data not shown). The *Pik3ca* Tg2 mice exhibited better glucose tolerance than WT mice at 8 weeks (Supplementary Fig. 2). The ratio of liver weight to body weight was significantly increased in the *Pik3ca* Tg mice compared to that of WT mice (Fig. 2A). The livers of 4 week-old *Pik3ca* Tg mice appeared slightly enlarged and light-colored, and they exhibited obvious fatty changes by 24 weeks (Fig. 2B). The Tg livers contained a greater volume of triacylglycerol than WT (Fig. 2C). The results of Western blotting revealed that Tg2 mice exhibited a relatively low activation of Akt and S6K as compared to Tg1 (Fig. 1B); however, hepatic triacylglycerol levels were clearly increased in the two lines Tg mice (Fig. 2C). Indeed, even Tg2 mice demonstrated an obvious fatty change in their livers by 24 weeks (Fig. 2B and D). These findings indicated that the constitutive expression of the *Pik3ca* N1068fs*4 transgene has a potential to establish *in vivo* hepatic steatosis. In addition, we found

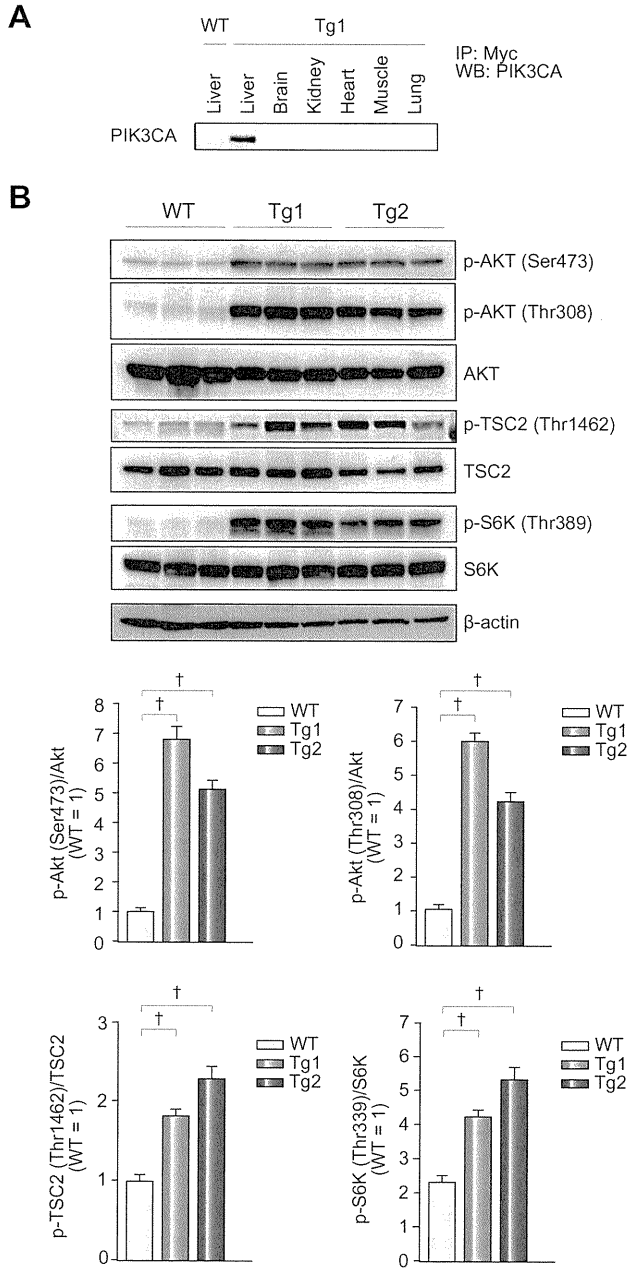

Fig. 1. Establishment of *Pik3ca* Tg mice. (A) Liver-specific expression of the mutant PIK3CA (N1068fs*4). (B) Immunoblots and quantification of the ratios of phosphorylated-Akt, TSC2, and S6K levels to total protein levels ($^{\dagger}p$ <0.05, ANOVA; post hoc test with WT).

that ALT levels in the *Pik3ca* Tg mice were higher than those of WT mice (Fig. 2E), suggesting the coexistence of liver damage. Next, we examined how the *Pik3ca* Tg liver induced unusual lipid accumulation. Because lipogenesis is mainly mediated by two major transcription factors, PPARγ and SREBP1C [24,25], we measured their expression levels and their target genes in Tg2 mice livers and observed the upregulation of PPARγ and its target aP2 but not of SREBP1C or its target FASN (Fig. 2F). Given the previous finding that activated PI3K signaling can induce steatosis through PPARγ [26], we speculated that PPARγ-dependent lipogenesis is a process responsible for hepatic steatosis in Tg mice. This was supported by the finding that the nuclear accumulation of the active form of SREBP1c protein was not increased by *Pik3ca* (N1068fs*4) expression (Supplementary Fig. 3). To emphasize this notion, we investigated whether the *in vitro* overexpression of *Pik3ca* (N1068fs*4) induced lipid accumulation and the activation of PPARγ-dependent transcription. The *in vitro* overexpression of *Pik3ca* (N1068fs*4) increased the concentration of triacylglycerol in BNL-CL2 cells, immortalized normal hepatocytes derived from a BALB/c mouse [27] (Fig. 2G), and upregulated *aP2* expression (Fig. 2H). These data indicated that the overexpression of *Pik3ca* (N1068fs*4) directly contributes to the enhanced lipogenesis, at least via activating PPARγ-dependent transcription. Given the important role of mTOR in lipogenesis through PPARγ, there is a possibility that the activation of mTOR signaling (Fig. 1B) contributes to deregulated lipogenesis through PPARγ signaling in the *Pik3ca* Tg liver [26].

Tumor formation without inflammation in the Pik3ca Tg mice

Regardless of the marked fatty changes and suggested liver damage, *Pik3ca* Tg livers did not exhibit cellular infiltration or fibrotic change even at 52 weeks of age (Fig. 3A and B), which means the expression of the *Pik3ca* transgene is not sufficient for progression to steatohepatitis in the mouse liver. We found that the inflammatory cytokine IL-1α and Fas ligand were highly expressed in the *Pik3ca* Tg liver than WT (Supplementary Fig. 4). Given the previous findings that these factors can be responsible for liver damage [28,29], the abnormal upregulation of IL-1α and Fas ligand in Tg livers may explain a part of the mechanisms of liver damage, whereas the entire molecular process inducing them remains unknown. Notably, macroscopic hepatic tumors developed in 94% of Tg1 mice (30/32) and 100% of Tg2 mice (11/11) at 52 weeks of age (Fig. 3C, left). Most of the tumors were hepatocellular adenomas containing abundant lipid droplets (Fig. 3C, right). Some tumors had rough surfaces and irregular shapes with necrosis and hemorrhaging (Fig. 3D, left) and microscopically demonstrated characteristics of HCC such as enlarged and hyperchromatic nuclei and trabecular patterns (Fig. 3D, right). HCC tissues did not always exhibit lipid accumulation as shown in Fig. 3D. As the *Pik3ca* Tg mice aged, hepatic tumors became increased in number and size, whereas no WT littermates developed any tumors (Fig. 3E). These data clearly indicate that the *in vivo* constitutive expression of *Pik3ca* (N1068fs*4) leads to hepatic tumor development. To assess the functional activity of PIK3CA (N1068fs*4) for tumorigenesis, we examined the *in vitro* transforming ability using BNL-CL2 cells. Remarkably, *Pik3ca* (N1068fs*4) expression did not stimulate colony formation of BNL-CL2 cells (Supplementary Fig. 5). In addition, we analyzed the phosphorylation level of Akt by the *in vitro* overexpression of *Pik3ca* genes including wild type, H1047R, or N1068fs*4 in 293T cells. The overexpression of *Pik3ca* (H1047R) possessing *in vitro* transforming capacity [13] resulted in strong phosphorylation of Akt, as previously reported (Supplementary Fig. 6) [30]. Conversely, the overexpression of *Pik3ca* (wild type) without any transforming capacity [13] resulted in lower phosphorylation of Akt. The mutant PIK3CA (N1068fs*4) induced phosphorylation of Akt, but the level was comparable to that of wild type, and less than that of H1047R (Supplementary Fig. 6). These findings suggested that *Pik3ca* (N1068fs*4), as compared to H1047R, has less capacity for activating Akt and little

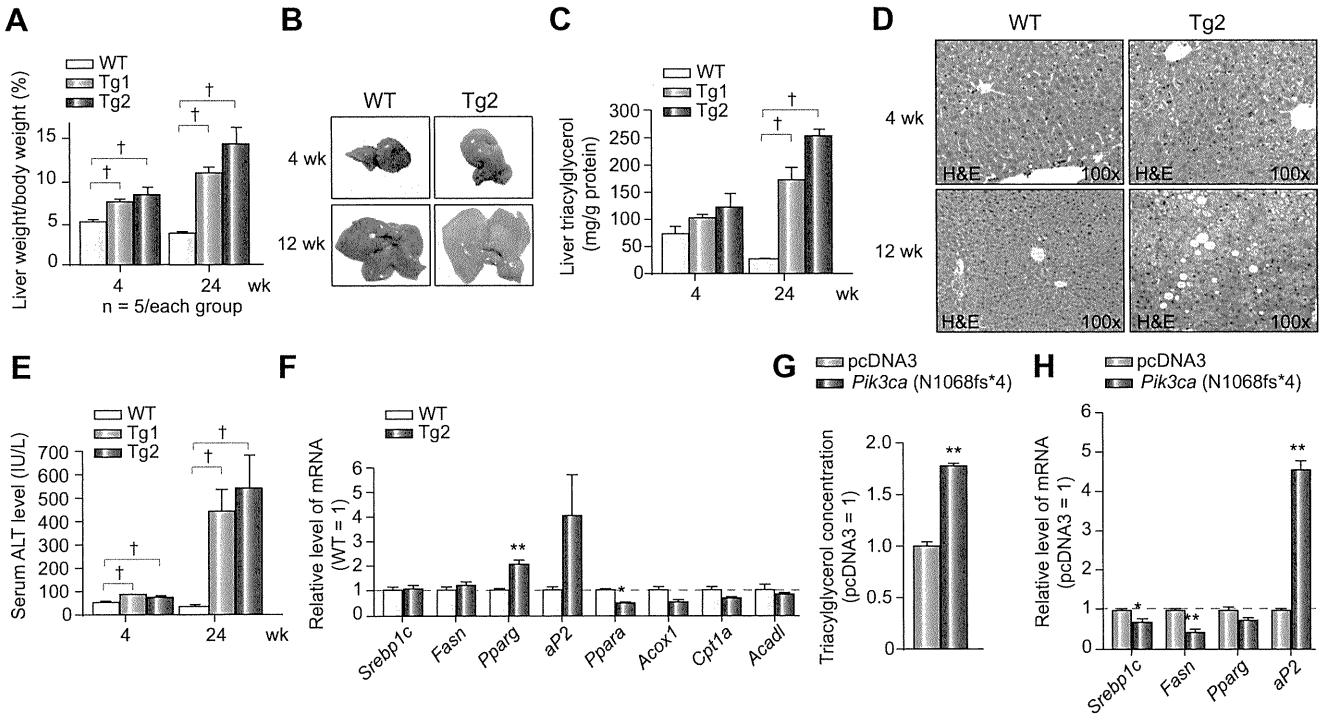

Fig. 2. Steatosis in the *Pik3ca* Tg liver. (A) Increased liver weight in *Pik3ca* Tg mice. (N = 5/group; †p <0.05, ANOVA; post hoc test with WT). (B) Representative liver images of WT and *Pik3ca* Tg mice. (C) High concentrations of intrahepatic triacylglycerol in the Tg mice (N >5/group; †p <0.05, ANOVA; post hoc test with WT). (D) H&E staining of livers from WT and *Pik3ca* Tg mice at 4 weeks (top) and 24 weeks (bottom) of age. (E) Higher serum ALT levels in the Tg mice (N = 5/group; †p <0.05, ANOVA; post hoc test with WT). (F) The expression of fat metabolism genes in the 4-week-old liver (N = 3–4/group; *p <0.05, **p <0.01, Student's t-test). (G) Cellular triacylglycerol levels and (H) the expression of lipogenesis-related genes in BNL-CL2 cells stably expressing *Pik3ca* (N1068fs*4) (N = 3/group; *p <0.05, **p <0.01, Student's t-test).

oncogenic activity in itself [13] and that there might be unknown factors promoting *in vivo* tumorigenesis in the *Pik3ca* Tg liver.

Downregulation of tumor suppressor genes in tumors derived from Pik3ca Tg livers

To further assess the related cellular signaling for tumorigenesis in the *Pik3ca* liver, we evaluated the activation of Akt, S6K, and Erk among the WT liver, non-tumor Tg liver, and tumor tissues from 52-week-old mice (Fig. 4A). Tumor tissues exhibited significantly enhanced activation of Akt compared to the Akt activation in non-tumor background or WT livers. We observed stronger phosphorylation of Akt in the non-tumor Tg liver than in WT livers, but the difference was not statistically significant as determined by ANOVA. Furthermore, the immunohistochemistry for phospho-Akt did not demonstrate clear differences between non-tumor livers and WT tissues. In contrast, the expression of *Myc-Pik3ca* was sustained in the non-tumor liver at 52 weeks (Supplementary Fig. 7). Those findings suggest the possibility that continuous activation of Akt induced by overexpressed *Pik3ca* is important for tumor formation in the Tg livers [31], whereas it remains unknown why Akt phosphorylation was attenuated in the non-tumor liver at 52 weeks despite the sustained expression of *Pik3ca* (Fig. 4A and Supplementary Fig. 7). In addition, the phosphorylation of S6K and Erk tended to be higher in Tg livers than in WT livers (Fig. 4A), but the difference became attenuated at 52 weeks compared to that at 4 weeks (Figs. 1B and 4A and Supplementary Fig. 8). These data do not exclude the possible role of these molecules in tumorigenesis in Tg livers but at least may emphasize the importance of Akt activation. Next, we examined the expression levels of genes involved in murine hepatotumorigenesis [32–34]. We observed decreased expression of four tumor suppressor genes, *Pten*, AT-rich interactive domain 5B (*Arid5b*), exportin 4 (*Xpo4*), and deleted in liver cancer 1 (*Dlc1*), in the tumor compared to the non-tumor background of *Pik3ca* Tg livers (Fig. 4B and Supplementary Fig. 9). PTEN protein levels were downregulated (Fig. 4C). To address whether the downregulation of *Pten* contributes to the tumorigenic activity in liver cells, we established *Pten*-depleted BNL-CL2 cells (Fig. 4D). *Pten*-depleted BNL-CL2 cells generated significantly more colonies in soft agar (Fig. 4E), indicative of enhanced tumorigenicity. These findings emphasize the possibility that the decreased expression of tumor suppressor genes has a certain role in tumorigenesis in the *Pik3ca* Tg liver. Importantly, the *in vitro* overexpression of mutant *Pik3ca* (N1068fs*4) only suppressed *Arid5b* expression but did not decrease the expression of *Pten*, *Xpo4*, or *Dlc1* in BNL-CL2 cells, indicating that certain additional mechanisms repressed their expression (Supplementary Fig. 10). Although several reports suggested a relationship between oxidative stress and hepatocarcinogenesis [35], the levels of hydrogen peroxide and lipid peroxidation were comparable between Tg and WT livers (Supplementary Fig. 11).

Tumors contain higher concentrations of OAs and palmitic acids (PAs) compared to the background tissues in the Pik3ca Tg liver

Recent intensive research has shed light into the significance of fatty acid (FA) as a potent biological stimulator of intracellular